Adv Polym Sci (2004) 166:113-171
DOI: 10.1007/b11350

Polyelectrolyte Complexes

Andreas F. Thünemann[1] · Martin Müller[2] · Herbert Dautzenberg[3] · Jean-François Joanny[4] · Hartmut Löwen[5]

[1] Fraunhofer Institute for Applied Polymer Research, Geiselbergstraße 69, 14476 Golm, Germany
E-mail: andreas.thuenemann@iap.fhg.de
[2] Institute of Polymer Research Dresden, Hohe Straße 6, 01069 Dresden, Germany
E-mail: mamuller@ipfdd.de
[3] Max Planck Institute of Colloids and Interfaces, Am Mühlenberg 1, 14476 Golm, Germany
E-mail: dau@mpigk-golm.mpg.de
[4] Institut Charles Sadron (CNRS UPR 022), 6 rue Boussingault, 67083 Strasbourg, France
E-mail: jean-francois.joanny@curie.fr
[5] Heinrich-Heine-Universität Düsseldorf, Universitätsstrasse 1, 40225 Düsseldorf, Germany
E-mail: hlowen@thphy.uni-duesseldorf.de

Abstract This chapter presents selected ideas concerning complexes that are formed either by oppositely charged polyelectrolytes or by polyelectrolytes and surfactants of opposite charge. The polyelectrolyte complexes (PECs), which are surfactant-free, form typical structures of a low degree of order such as the ladder- and scrambled-egg structures. In contrast, polyelectrolyte-surfactant complexes (PE-surfs) show a large variety of highly ordered mesomorphous structures in the solid state. The latter have many similarities to liquid-crystals. However, as a result of their ionic character, mesophases of PE-surfs are thermally more stable. Both, PECs and PE-surfs can be prepared as water-soluble and water-insoluble systems, as dispersions and nanoparticles. A stoichiometry of 1:1 with respect to their charges are found frequently for both. Structures and properties of PECs and PE-surfs can be tuned to a large extent by varying composition, temperature, salt-concentration etc. Drug-carrier systems based on PECs and PE-surfs are discussed. Examples are complexes of retinoic acid (PE-surfs) and DNA (PECs). A brief overview is given concerning some theoretical approaches to PECs and PE-surfs such as the formation of polyelectrolyte multilayers.

Keywords Polyelectrolyte-surfactant complexes · Polyelectrolyte-polyelectrolyte complexes · Polyelectrolyte-colloid complexes · Polyelectrolyte-multilayers · Polyelectrolyte nanoparticles · Retinoic acid

1 Introduction

An increasing number of articles on polyelectrolyte complexes reflect the growing scientific and industrial interest in this field. Some reviews are given in [1-7]. Polyelectrolyte complexes can be roughly divided into two types: The first type (PECs) are complexes of cationic and anionic polyelectrolytes. The second type (PE-surfs) are complexes of anionic polyelectrolytes and cationic surfactants and those of cationic polyelectrolytes and anionic surfactants. In its most simple form complex formation is observed when the two oppositely charged species-polyelectrolyte and polyelectrolyte or polyelectrolyte and surfactant are mixed in aqueous solution. But a number of different procedures to form PECs and PE-surfs have been developed. For example, multilayer films of PECs on solid surfaces were prepared by chemisorption from solution. This is well-known as the layer-by-layer technique and synonymously as electrostatic self-assembly [3]. The first experiments on multilayers made of oppositely charged polyelectrolytes were carried out by Decher et al. [8]. The resulting superlattice architectures of the PECs are somewhat fuzzy structures. Some reasons are i.) the build-up process of consecutive adsorption of polycations and polyanions is kinetically controlled and ii.) the polyelectrolytes are typically flexible molecules. But the absence of crystallinity in these films is expected to be beneficial for many potential applications [09]. Meanwhile the layer-by-layer method has been extended to other materials such as proteins [10, 11] and colloids (e. g. inorganic nanosheets of the clay mineral montmorillonite) [12]. Moreover, hollow nano- and microspheres are obtained via layer-by-layer adsorption of oppositely charged polyelectrolytes on template nano- and microparticles [13, 14].

The complex formation of PECs and PE-surfs is closely linked to self-assembly processes. A major difference between PECs and PE-surfs can be found in their solid-state structures. PE-surfs show typically highly ordered mesophases in the solid state [15] which is in contrast to the ladder and scrambled-egg structures of PECs [2]. Reasons for the high ordering of PE-surfs are i) cooperative binding phenomena of the surfactant molecules onto the polyelectrolyte chains [16-18] and ii) the amphiphilicity of the surfactant molecules. A further result of the cooperative zipper mechanism between a polyelectrolyte and oppositely charged surfactant molecules is a 1:1 stoichiometry. The amphiphilicity of surfactants favors a microphase separation in PE-surfs that results in periodic nanostructures with repeat units of 1 to 10 nm. By contrast, structures of PECs normally display no such periodic nanostructures.

2 Polyelectrolyte-Polyelectrolyte Complexes (PECs)

In many practical uses PEC formation takes place under conditions, where structure formation is mainly determined by the fast kinetics of this process,

concealing the effects of different parameters of influence such as the mixing regime, medium conditions and macromolecular characteristics of the polyelectrolytes. The investigation of PEC formation in highly diluted aqueous solutions offers a much better chance of elucidating the general features of this process and to examine the consequences by varying the combination of polyelectrolytes and the formation conditions. After giving a brief description of the physical background of PEC formation and the basic findings regarding soluble PECs, we will focused on PEC formation in highly aggregating systems.

2.1 Physical Background of PEC Formation

The mixing of solutions of polyanions and polycations leads to the spontaneous formation of interpolymer complexes under release of the counterions. Complex formation can take place between polyacids and polybases, but also between their neutralized metal and halogenide salts. For free polyelectrolyte chains the low molecular counterions are more or less localized near the macroions, in the case of high charge densities, particularly because of counterion condensation. The driving force of complex formation is mainly the gain in entropy due to the liberation of the low molecular counterions. However, other interactions such as hydrogen bonding or hydrophobic ones may play an additional part. From the energetic point of view, PEC formation may even be an endothermic process, because of the elastic energy contributions of the polyelectrolyte chains, impeding the necessary conformational adaptations of the polymer chains during their transition to the much more compact PEC structures.

The reaction of polyelectrolyte complex formation can be described by the following equation:

$$(>-A^-c^+)_n+(>-C^+a^-)_m \Leftrightarrow (>-A^-C^+)_x+(>-A^-c^+)_{n-x} + (>-C^+a^-)_{m-x}+xa^-+xc^+ \quad (1)$$

where A^-, C^+-are the charged groups of the polyelectrolytes, a^-, c^+-counterions, n, m-number of the anionic and cationic groups in solution, n/m or m/n=X-molar mixing ratio, θ=x/n, n<m or θ=x/m, m<n, θ-degree of conversion. The degree of conversion determines whether the ionic sites of the components in efficiency are completely bound by the oppositely charged polyelectrolytes or whether low molecular counterions partly remain in the complex. Another characteristic quantity is the overall composition of the PEC structures at any mixing ratio. Even if the stoichiometry of the ionic binding is 1:1, the major component may be bound in excess, leading to an overcharging of the PEC particles.

PEC formation leads to quite different structures, depending on the characteristics of the components used and the external conditions of the reac-

tion. As borderline cases for the resulting structures of polyelectrolyte complexes two models are discussed in the literature [19]:

- The ladder-like structure, where complex formation takes place on a molecular level via conformational adaptation (zip mechanism),
- and the scrambled egg model, where a high number of chains are incorporated into a particle.

Beside the determination of the PEC stoichiometry, the detailed characterization of the PEC structures is the main objective in understanding the effects of various parameters on the course of complex formation and the resulting properties of the PECs.

2.2 Water-Soluble PECs

Comprehensive and systematic studies on soluble PECs started with the pioneering work of the groups of Kabanov [20-22] and Tsuchida [23-25]. They could show that under appropriate salt conditions, PEC formation between polyions with weak ionic groups and significantly different molecular weights in non-stoichiometric systems results in soluble complexes. Such PECs are structured according to the ladder model, consisting of hydrophilic single-stranded and hydrophobic double-stranded segments. Predominantly carboxylic groups containing polyanions were used in combination with various polycations. The presence of a small amount of salt enables rearrangement and exchange processes and shifts the reaction more to thermodynamic equilibrium, leading to a uniform distribution of the short chain components among all long chains of the counterpart. Stop flow measurements [26] showed that PEC formation takes place in less than 5 μs, nearly corresponding to the diffusion collision of the polyion coils. The further addition of salt leads at first to a shrinking of the PECs due to the shielding of their charges by the electrolyte. When a critical salt concentration is exceeded, a disproportionation of the short guest chains occurs, leading to completely complexed, precipitating species and pure host polyelectrolyte chains in solution [27-29]. At still higher salt concentration the precipitate dissolves again and both components exist as free polyelectrolyte chains in solution. Similar effects can be induced by changes of the p-H-value [21].

While at low ionic strength the PECs possess a high stability, they are able to take part in polyion exchange and substitution reactions at higher ionic strengths. Especially, the addition of a component of higher molecular mass or stronger ionic groups results in substitution reactions [30, 31]. Therefore, one should always be aware that polyelectrolyte complexes are "living systems", which may respond very sensitively to changes of their environment.

2.3
Dispersions of Highly Aggregated PEC Particles

The preparation of soluble PECs requires special conditions. Most of the practical applications do not meet such demands. Particularly, PEC formation between strong polyelectrolytes results in highly aggregated or macroscopic flocculated systems. However, in extremely diluted solutions the aggregation process stops on a colloidal level, offering the possibility to study these dispersions of PEC particles in detail. We focused our interest on the investigation of the stoichiometry and structure of such PECs, looking especially for the general effects of various macromolecular and external parameters.

2.3.1
Stoichiometry of the PECs

2.3.1.1
Stoichiometry of Ionic Binding

The first step in determining the composition of the PEC particles is to find the stoichiometry of the ionic binding, i.e. of the degree of conversion. Well-established techniques of studying the endpoint stoichiometry of PEC formation are turbidity, potentiometry, conductivity, electrophoretic light scattering, and colloidal titration. A maximum or a breakpoint of the measured quantity indicate the endpoint of the reaction of complex formation (for details of these methods see Review [32]). For strong polyelectrolytes in most cases a 1:1 endpoint stoichiometry was found. Some of these techniques also allowed us to determine the stoichiometry as a function of the molar mixing ratio X of the oppositely charged components. Micheals et al. [33] studied PEC formation between sodium poly(styrene sulfonate) (NaPSS) and poly(4-vinylbenzyl-trimethylammonium chloride) (PVBTACl) by conductometry. A comparison of the conductivity of the PEC solutions with that of control solutions containing the same amount of low molecular counterions according to a 1:1 reaction and the remaining excess polyelectrolyte, proved that the component reacted completely under full release of the low molecular counterions. The same conclusion could be drawn from UV spectroscopy and potentiometry with a chloride sensitive electrode for the UV-active polyanion NaPSS in combination with poly(diallyldimethylammonium chloride) (PDADMAC) or its copolymers with acrylamide [34]. These investigations were carried out using deionized water as a solvent. NMR studies on the same polycations in combination with different NaPSS samples revealed, for NaPSS of higher molecular masses, a full binding, especially at higher ionic strength [35]. The full binding of the component in deficiency even for strong mismatching of the charge densities of the components, suggests a more smoothed charge neutralization than a strictly located salt binding.

2.3.1.1.1
Overall Composition

While for the ionic binding the 1:1 stoichiometry seems to be the rule in the case of strong polyelectrolytes ζ-potential measurements by electrophoretic light scattering [36, 37] revealed a strong overcharging for non-stoichiometric mixing ratios. In [38], viscometry was used to determine the total composition of the PEC particles between NaPSS and DADMAC-acrylamide copolymers. The stoichiometric factor decreases from ~1.5 at low mixing ratios to 1 at 1:1 mixing of charged groups. Similar results were obtained by analyzing the complex solutions and the supernatants by analytical ultracentrifugation using an UV-detector [39]. Also chromatographic techniques [40, 41] and gel electrophoresis [42] were employed in this regard.

2.3.2
Structure of the PECs

2.3.2.1
PEC formation in pure water

At first PEC formation in pure water will be considered. Electron and X-ray absorption microscopy showed that PEC formation leads to polydisperse systems of nearly spherical particles [32, 34]. To study the PEC structure in detail static and dynamic light scattering were used. Static light scattering in its traditional manner of data analysis provides information about the weight average of the particle mass and the z-average of the square of the radius of gyration. A more detailed interpretation of the shape of the scattering functions by comparison with model calculations for various structures [43-45] yields additional information about the structure type and polydispersity and allows the calculation of the structural density (reciprocal of the degree of swelling). Dynamic light scattering yields, by the cumulant fit of the correlation function the z-average of the diffusion coefficient and via the Einstein-Stokes equation, the hydrodynamic radius (for details see [46]). The ratio between the radius of gyration and the hydrodynamic radius is a structure sensitive parameter and varies from ρ_s=0.775 for monodisperse spheres to values much higher than unity for elongated structures. A Laplace transform of the correlation function directly provides the distribution function of the decay constants, and for spheres the distribution of radii [47].

The findings of light scattering studies on PEC formation between a variety of different polyanions and polycations [32, 34, 48-50] can be summarized as follows:

PEC formation in a concentration range of the component solutions below $1 \cdot 10^{-3}$ g/mL resulted in stable dispersions of PEC particles when non-stoichiometric mixing ratios are used. In general, the scattering functions of the PECs could be well fitted by the model of polydisperse systems of homo-

geneous spheres, using a logarithmic distribution to describe the polydispersity of radii. Taking into account the polydispersities obtained by static light scattering, the results of dynamic light scattering confirmed nicely the model used. Together with the findings about PEC stoichiometry this leads to the conclusion that the sphere-like PEC particles consist of a charge neutralized core, surrounded by an electrostatically stabilizing shell of the excess component.

The structural parameters of the PECs (mass, size, structure density) changed only slightly with the molar mixing ratio X up to about X=0.9. Mass and size of the complexes decreased somewhat in such a way that the structure density remained nearly constant. The decrease in PEC particle mass can be explained by the consumption of the excess component. Therefore, not a growing of the PEC particles, but the generation of new particles is the dominating process with increasing mixing ratio. Secondary aggregation and macroscopic flocculation occurred when the 1:1 mixing ratio is approached.

Even in extremely diluted systems ($<1\times10^{-5}$ g/ml) the PEC particles consist of several hundred single polyelectrolyte chains. The level of aggregation increases strongly with the rising concentration of the component solutions up to several thousand chains per particle [50].

For strong polyelectrolytes and suitable charge densities of the components the structure density of the PECs is high and ranges normally from 0.3 to 0.7 g/mL, indicating very compact structures. Stronger mismatching of the charge distances of the components results in higher degrees of swelling [34, 48, 49].

By contrast to expectations (from the thermodynamic point of view [51]), PEC formation between PDADMAC and a series of NaPSS of different molecular masses (8000 to 1million g/mol) did not reveal systematic changes of the structural parameters with variation of the molecular masses of NaPSS. Most likely, in pure water PEC formation is mainly governed by the kinetics of this process, leading to frozen structures, which are far from thermodynamic equilibrium. This statement is supported by the findings on preferential binding from a mixture of polyanions during the addition of a PDADMAC solution [52, 53]. An equal binding of both kinds of polyanions or even a preferential binding of the thermodynamically handicapped component (weaker ionic groups or lower molecular weight) was found. Especially, a strong favoring of a low molecular mass NaPSS in competition with a high molecular mass NaPSS was observed in pure water. Only an appropriate amount of NaCl in the solutions shifted the preferential binding to the thermodynamically favored component.

2.3.3
Effect of Salt

2.3.3.1
PEC Formation in the Presence of Salt

Because it weakens the electrostatic interaction and enables rearrangement processes salt should play a decisive part in the formation of highly aggregated PECs similar to the role of salt in the formation of soluble PECs. This topic has been addressed in detail in [54, 55, 56, 57]. The presence of a small amount of NaCl led to a dramatic decrease of the level of aggregation for PECs between NaPSS and PDADMAC by nearly two orders of magnitude. Higher ionic strengths caused secondary aggregation and again a strong increase in PEC masses and sizes. Therefore, the level of aggregation can also be controlled by the amount of salt during complex formation. In contrast to PEC formation in pure water, a remarkable increase in the aggregation level with a rising mixing ratio X was observed. PEC formation between NaPSS and a DADMAC-acrylamide copolymer with 47 mol% DADMAC in the presence of NaCl resulted in a strongly swollen PEC structures up to a mixing ratio X=0.5, where a collapse to highly aggregated and compact particles occurred. Very recent studies on PEC formation between NaPSS and well-defined copolymers between DADMAC and *N*-methyl-*N*-vinyl-acetamide (MVA) of various compositions revealed the same pattern, as shown in Fig. 1. While at 75 mol% of DADMAC complex formation is very similar to the case of PDADMAC, for the sample with 25 mol% DADMAC a strong

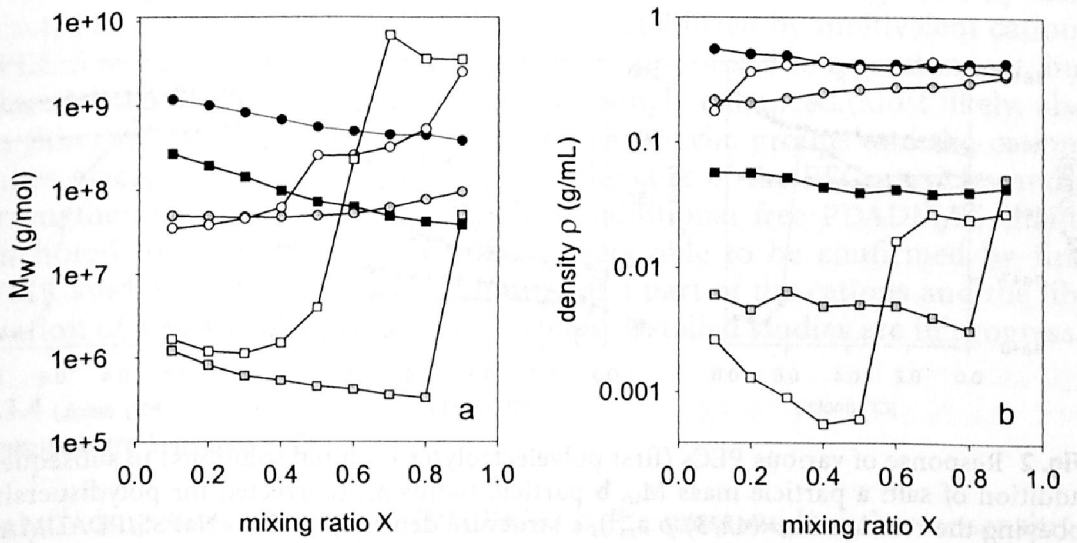

Fig. 1 Particle mass M_w and structure density ρ of PECs between DADMAC-MVA-copolymers (M_w=100 kDa) and NaPSS (M_w=66 kDa) in dependence on mixing ratio X:1 (●) copolymers with 75 mol% DADMAC, 2 - (■) copolymer with 25 mol% DADMAC, *black* - pure water, *grey* - 0.01 N NaCl, *white* - 0.1 N NaCl

increase in particle mass and structure density was found in 0.1 N NaCl at X=0.5.

2.3.3.2 Subsequent Addition of Salt

Comprehensive studies of various PEC systems [48, 55-058] revealed that the response of polyelectrolyte complexes to the addition of NaCl is be very different, strongly depending on the used polyelectrolyte components. The general tendencies may be summarized as follows:

PECs between strong polyelectrolytes shows secondary aggregation up to macroscopic flocculation (systems 1 and 2 in Fig. 2). The colloidal salt stability decreases drastically with an increasing mixing ratio. This can easily be understood by the corresponding decrease in the thickness of the stabilizing shell of the excess component and in the degree of overcharging. For the complex NaPSS/PDADMAC dissolution did not occur up to an ionic strength of 4 mol/L. The structure density remained nearly constant. By contrast, PECs of polyanions with carboxylic groups swelled and dissolved completely at a critical salt concentration (PEC 3 in Fig. 2), where this salt concentration depends on the charge densities of the components.

The colloidal salt stability can be improved by using double hydrophilic block or graft copolymers with neutral water-soluble chains [59-62], as shown in PEC 4 in Fig. 2. While, for a stabilization of the PEC particles during complex formation in pure water close to the 1:1 mixing ratio, short PEG chains (2 kDa) are sufficient, long blocks were found to be necessary to stabilize PECs against salt induced aggregation. In the first case the lowering

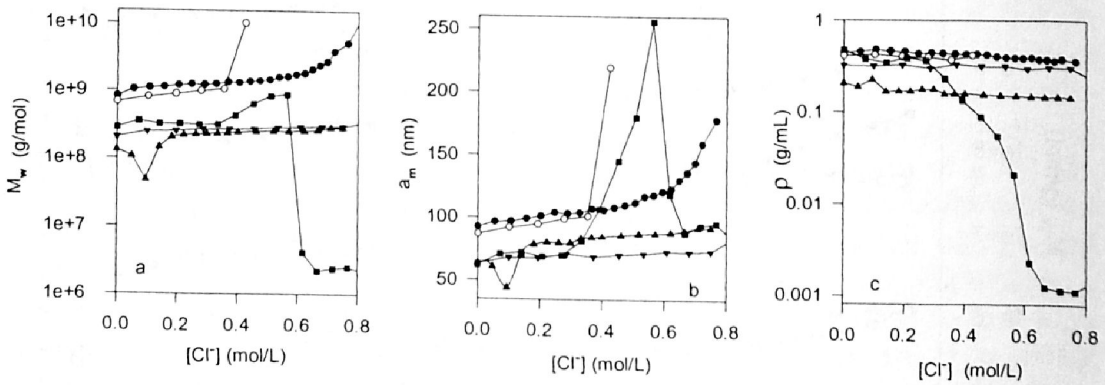

Fig. 2 Response of various PECs (first polyelectrolytes in initial solutions) to subsequent addition of salt: **a** particle mass M_w, **b** particle radius a_m (corrected for polydispersity, obeying the relation $M_w=(4\pi/3)\ \rho\ a_m^3$), **c** structure density ρ: 1(●) - NaPSS/PDADMAC, X=0.3, 2(○) - NaPSS/PDADMAC, X=0.6, 3(■) - DADMAC-acrylamide copolymer (47 mol% DADMAC)/NaPMA X=0.6, 4(▼) - DHP2 (block copolymer of poly(2-acrylamido-2-methyl-1-propanesulfonic acid) and poly(ethylene glycol), PEG block length 10 kda)/PDADMAC, X=0.6, 1-4: addition of NaCl, 5(▲) - DADMAC-acrylamide copolymer (47 mol% DADMAC)/Na-PMA, X=0.6, addition of $CaCl_2$

of the flocculation rate of the PEC particles enables the passage of this critical region during the short time of the experiment.

For recording the correct scattering curves during salt induced aggregation, it was necessary to wait up to one hour after the dosage step before the scattering intensities became sufficiently stable. Especially at low ionic strengths the process of secondary aggregation is slow.

Using a DAWN EOS multiangle light scattering instrument additionally equipped with a cylindrical cell with plan-parallel windows as a matching bath, time-resolved measurements were carried out [63]. The time dependent changes were detected after the addition of different amounts of NaCl to a complex between Na-poly(methacrylate) (NaPMA) and PDADMAC. In 0.1 N NaCl the aggregation process was completed only after 20 hours, while in 0.2 N NaCl the final state was reached in half an hour when the PEC began to precipitate. However, the dissolution process above the critical NaCl was completed in fractions of a second.

Very slow long-term changes were also observed in the investigations of the exchange processes of low molecular mass for high molecular mass NaPSS or NaPMA for NaPSS [53]. A complete exchange took place after 2 months in the presence of 0.1 N NaCl.

The occurrence of such long-term changes in salt-containing systems has to be taken into account in all applications of polyelectrolyte complexes.

Very interesting results were obtained in studies on the effect of multivalent added salts ($CaCl_2$, $MgCl_2$, $AlCl_3$, and FeCl3) [63]. NaPMA was used as the polyanion to estimate both the colloidal stability and the stability of the ionic binding. If the multivalent ion is the counterpart of the component in excess strong secondary aggregation took place, obviously caused by additional complexation of the carboxylic groups of the stabilizing shell. By contrast, PECs with NaPMA in deficiency were stabilized by multivalent cations (PEC 5 in Fig. 2). Secondary aggregation is suppressed to a great extent, but also the stability of the ionic binding is strongly enhanced. Most likely, also in this case complex formation between carboxylic groups and the cations takes place, leading to a stabilization of the core of the PEC particles and a strengthening of the stabilizing shell by additional free PDADMAC chains anchored in the core. This hypothesis were able to be confirmed by first NMR studies, which proved the binding of a part of the cations and the liberation of a part of the polycationic groups. Detailed studies are in progress.

2.3.4
Temperature Sensitive PECs

Poly(*N*-isopropylacrylamide) (PNIPAM) is the most studied thermosensitive polymer in aqueous media. It is soluble in water at low temperatures but becomes insoluble when the temperature is increased above a certain temperature (~32 °C) (lower critical solution temperature), which is related to the coil-to-globule transition [64, 65]. In the case of a polymer network, a volume change occurs reversibly within a narrow temperature range. The properties of such microgels can be varied to a great extent by the introduction

of ionic groups [66-69]. Thermosensitive gels have mostly been prepared by covalent cross-linking. However, polyelectrolyte complex formation between ionically modified temperature sensitive polymers should offer a promising new route in the preparation of tailor-made gel particles on a nanometer scale. Recent studies [70] on PEC formation between ionically modified PNIPAM has demonstrated that nearly monodisperse, sphere-like complex particles in a 100 nm scale can be prepared, which show a temperature controlled, reversible swelling-deswelling behavior by nearly a factor 10 at about 35 °C.

2.4 Potential Applications of PECs in Solution

Polyelectrolyte complexes can be prepared in a desired range of mass, size and structure density. The behavior of the PECs can be controlled by external parameters such as the ionic strength, the pH of the medium or the temperature. Therefore, such complexes should be of great interest as potential carrier systems for drugs, enzymes, or DNA because charged species can easily be integrated into the complex particles.

2.4.1 *Polyelectrolyte-Enzyme Complexes*

Comprehensive investigations have been carried out about the complex formation between proteins and polyelectrolytes (see reviews [71-73]). Kabanov described in [22, 74] a protection-activation mechanism for enzymes by a pH induced solution-precipitation process of their complexes with polyelectrolytes. The direct coupling of an enzyme to a polyelectrolyte often leads to a strong loss of its activity. Therefore, in [74] it was proposed to immobilize enzymes in a complex matrix of synthetic polyelectrolytes. The basic idea consists of the fact that PEC formation can be carried out under optimal pH conditions for incorporation of an enzyme into the complex and then the pH can be adjusted to the pH value for the highest activity without its release from the PEC matrix. The immobilization procedures were optimized regarding the pH, nature and molecular mass of the components as well as the mass ratio enzyme/polyelectrolytes for trypsin [75], lipases [76] and amyloglucosidase [77], yielding activities of the immobilized enzymes between 50 and 90% of the uncomplexed enzyme. In [77] the complex solution was additionally entrapped in poly(vinylalcohol) gel particles, enabling an easy handling of the enzyme in industrial applications and repeated uses without loss of activity.

2.4.2
DNA-Polycation Complexes

More than 6000 diseases are known to be caused by a single gene defect. While classical medicine can only cure the symptoms, gene therapy offers the possibility of correcting such defects by introducing DNA, or their fragments, into cells. One of the challenging problems in this respect is the development of appropriate carrier systems which guarantee a high rate of cell transfection, but a low mortality of the cells. A good survey of this area of research is given in [78]. DNA or oligonucleotide complexes with polycations have proven to be promising gene delivery systems [79, 80]. A serious problem results from their low colloidal stability, particularly near a 1:1 mixing ratio of anionic to cationic groups and under physiological salt conditions. The use of double hydrophilic polycations improved the situation decisively [81-86].

However, in many cases the high level of aggregation of the complexes remained a great disadvantage, especially for oligonucleotides, because it causes the introduction of several thousands DNA fragments into one cell. Carrying out PEC formation under conditions according to the generation of soluble PECs, the aggregation level could be drastically reduced [87].

2.4.3
PLL/Polyanion Complexes

Polypeptide/polyelectrolyte complexes are interesting for fundamental research on biomolecular recognition on the conformation level and for applications such as pharmaceutical drug carriers. Several non-biogenic polyanion solutions were mixed in excess with Poly(L-lysine) (PLL) solutions at a constant pH=6 to give negatively charged nonstoichometric dispersed PEC, i.e., all PLL is expected to be consumed by the polyanion. At this pH prior to mixing PLL adopts the random coil conformation. By CD spectroscopy it was possible to probe the influence of several polyanions on its conformation. In Fig. 3 CD spectra of selected PECs composed of PLL and the polyanions poly(vinyl sulfate) (PVS), poly(styrenesulfonate) (PSS), poly(acrylic acid) (PAC), poly(maleic acid-*co*-ethylene) (PMA-E) and poly(maleic acid-*co*-α-methylstyrene) (PMA-MS) are given. Generally, a negative CD band around 190 nm can be diagnostically assigned to random coil conformation and the 222/206 nm doublet ($n-\pi^*$, $\pi-\pi^*$ transitions) to the α-helical conformation of polypeptides. The latter could be seen in the PLL complexes with PAC, PMA-E and PVS. In contrast PMA-MS and PSS showed similar CD spectra like that of the uncomplexed PLL at pH=6. No definite rule could be derived from these findings, since the strong and supposedly more extended PVS induces the α-helix in contrast to the also strong PSS. Furthermore the weak and less extended PAC and PMA-E (the head/head adduct of PAC with different charge distances) tended to be α-helix formers. Similar conformation directing results were found for PLL/PAC complexes by Shinoda [88], who claimed a stoichiometric reaction between PLL and PAC and

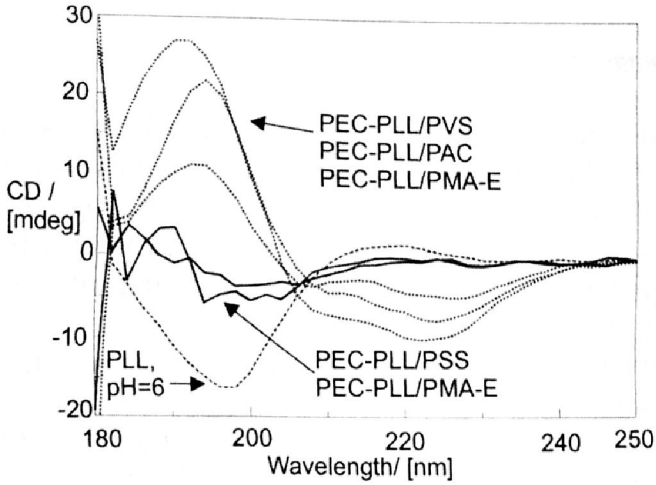

Fig. 3 CD spectra of negatively charged nonstoichometric PECs consisting of PLL and of different polyanions (PA, indicated in the plot) mixed at n−/n+=2.0 (c_{PLL}= c_{PA}=0.001m, pH=6) and of PLL at pH=6

furthermore a left-handed super helix of PAC around the right-handed α-helix of PLL. Since both PMA-MS and PSS did not influence the PLL conformation at pH=6, it might be concluded, that aromatic ring containing polyanions cannot bind PLL in the α-helical state due to preassociated structures of these polyanions.

2.5 Surface Modification by PECs

Surface modification by polyelectrolytes and PECs has been established for many years [89, 90]. For example, the interaction between the oppositely charged polymers poly(diallyldimethylammonium chloride) and poly(maleic acid-*co*-methylstyrene) in the presence of cellulose leads to a strong surface modification [91]. Model systems that are based on PEC nanoparticles with a small size distribution were used for the investigation of their adsorption on different surfaces [92]. The deposition of PEC particles on silica surfaces has been characterized by in-situ-ATR-FTIR, which has been shown to be suitable for monitoring adsorption processes at the liquid/solid interface on the molecular level [93], and SEM methods [94]. In Fig. 4 there are representative in-situ-ATR-FTIR spectra on the adsorption of PECs consisting of PDADMAC/PMA-MS (n−/n+=0.6) on a silicon substrate, which has been premodified by a six layered polyelectrolyte multilayer assembly of poly(-ethyleneimine) (PEI) and poly(acrylic acid) (PAC). Prominent IR bands of the PEC like the ν(CH) and the $\nu(COO^-)$ evolve with increasing adsorption time paralleled by the incline of the negative ν(OH) band, which is due to the adsorption induced subsequent water removal from the surface. The integrals of these bands are given in Fig. 5 showing that the adsorption kinetics of the PECs is rather slow and takes more than two hours for completion of the surface coverage. A representative SEM image of these adsorbed PEC-

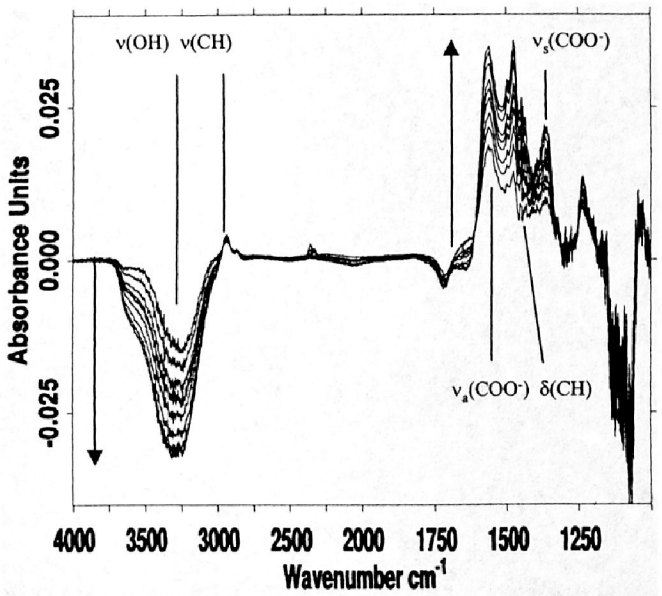

Fig. 4 in-situ-ATR-FTIR spectra monitoring the adsorption of PEC particles composed of PDADMAC/PMA-MS-0.6 at a negatively charged multilayer modified surface in dependence on adsorption time (c_{PEC}=0.0032m, pH=6)

particles composed of PDADMAC and PMA-MS on the negatively charged surface is given in Fig. 6. There, individually adsorbed droplet-like particles in the range of 200-1000 nm with a certain distribution maximum around 450 nm were observed with slight tendencies to fusion on the surface [95]. The shape of these particles appeared to be hemispherical, whereas that of

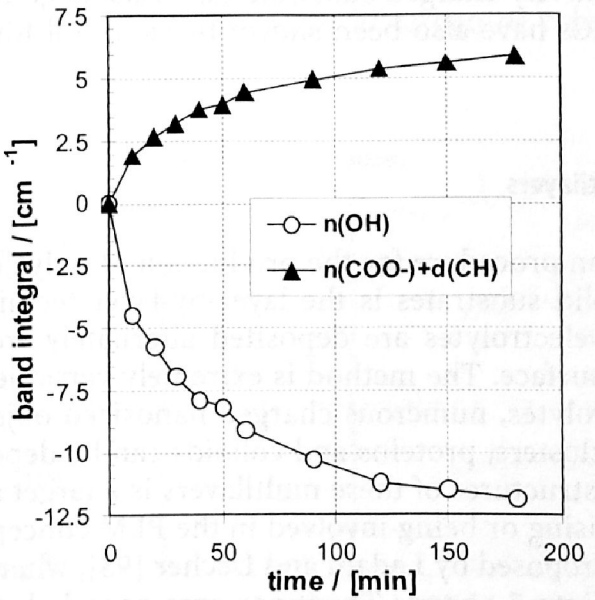

Fig. 5 Integrated areas of the ν(OH) band (water) and the composed band of ν(COO^-) and ν(CH) (PEC particles) (from Fig. 4) as a linear scale for PEC surface coverage in dependence of adsorption time

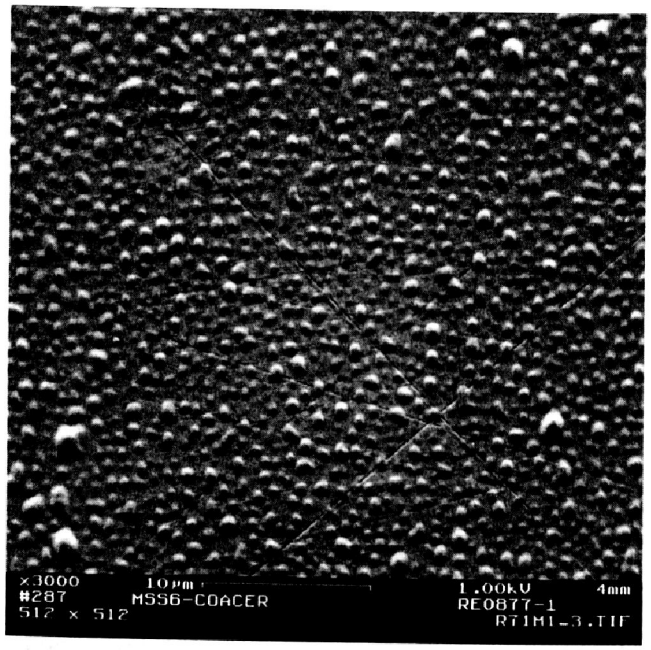

Fig. 6 Adsorbed positively charged PEC particles composed of PDADMAC and PMA-MS (n−/n+=0.6, $c_{Pol,\,tot}$=0.0032 m) on a negatively charged surface

PDADMAC and poly(maleic acid-*co*-propylene) (PMA-P) were found to be more deformed and disk-like.

From this it was concluded that PEC nanoparticles can be somewhat analogous to latex systems, lacking, however, in an equivalent stability at the respective higher solid contents. The possibility of surface charge modification of inorganic negatively charged substrate materials is given by the choice of the PEC [96]. PECs have also been shown to be useful for flocculation processes [97].

2.6 Polyelectrolyte-Multilayers

The most common procedure for the production of polyelectrolyte multilayers (PEMs) at solid substrates is the layer-by-layer technique [3]. Cationic and anionic polyelectrolytes are deposited alternately from aqueous solutions to a target surface. The method is extremely versatile because, in addition to polyelectrolytes, numerous charged nanosized objects such as molecule aggregates, clusters, proteins and colloids can be deposited as multilayers. The internal structures of these multilayers is a target area of interest for working groups using or being involved in the PEM concept.

A model was proposed by Ladam and Decher [98], whereby the multilayer phase is divided into 3 zones : The inner core zone I close to the substrate consists of few (4-5) inhomogeneously adsorbed PEL layers and zone II is a homogeneous isotropic layer phase, in which a 1:1-stoichometry and high entanglement prevails. The outermost zone III consists again of a few (4-5)

PEL layers whose charges are not completely compensated. The uppermost PEL layer it is claimedis released into zone II, when a new oppositely charged polyelectrolyte is adsorbed on top. The isotropic unordered internal structure of zone II might be described theoretically by the Random-Phase-Approximation (RPA) [99], according to which the complexed and entangled PELs are modeled by Gaussian coils. This model was supported by Castelnovo and Joanny [100], who gave a mechanism for the overcharging as the driving force for the multilayer built up.

Generally, Zone (II) of PEMs is seen to be identical with the inner zone of dispersed polyelectrolyte complexes (PECs, see above), whereas the zone III of PEMs might be analogous to the outer shell zone of PECs.

2.6.1
Dissociation degree of PEMs and PECs

In Fig. 7 IR spectra of PEM-5 and PEM-6 of PEI/PAC and of solution cast PECs of PEI/PAC (n−/n+=0.80 and 1.25) prepared at pH=4 (PAC) and 6 (PEI) are shown. Both the spectrum of the polycation terminated PEM-5 and that of PEC-0.8 of PEI/PAC were comparable, since they contain PEI in excess. The PEM-5 spectrum showed only a minor ν(C=O) and a major $\nu(COO^-)$ band, since all COOH groups were consumed by the overlaying PEI layer, whereas the PEM-6 spectrum showed a major ν(C=O) and minor $\nu(COO^-)$ band. From these two bands the dissociation degree of PAC can be calculated using the relation

$$\alpha_{IR} = A_{\nu(COO^-)} / (1.74 \cdot A_{\nu(C=O)} + A_{\nu(COO^-)}) \quad (2)$$

which was described in [93]. Using this formula, the α_{IR} values of differently deposited PAC containing multilayers or PECs can be calculated, which will

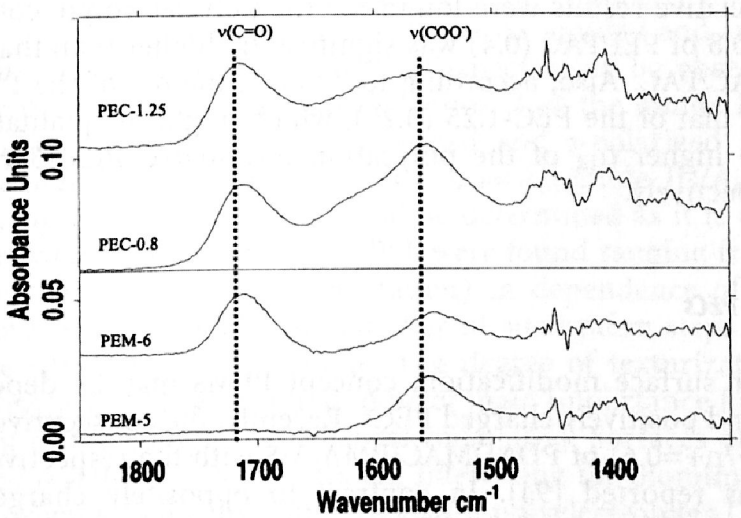

Fig. 7 ATR-FTIR spectra of the consecutively adsorbed PEM-5 and PEM-6 and of solution casted PECs of PEI/PAC with n−/n+=0.80 (PEC-0.8) and 1.25 (PEC-1.25)

Table 1 Dissociation degree α_{IR} of several samples of PEMs and PECs composed of PAC and PEI or PDADMAC deposited or mixed at pH 6 (PEI) and 4 (PAC)

	α_{IR} PEM-5	α_{IR} PEM-6	α_{IR} PEC-0.80	α_{IR} PEC-1.25
PEI/PAC	0.89±0.03	0.26±0.03	0.40±0.05	0.20±0.05
PDADMAC/PAC	0.70±0.03	0.13±0.03	low	low

be reported more detailed in [101]. In the Table 1 α_{IR} values are given for the samples introduced in Fig. 7. Significantly, for the polycation terminating PEM-5 of PEI/PAC the dissociation degree gets close to unity, which means all COOH groups are deprotonated by the reacting ammonium groups of the polycation. Whereas for the PAC terminating PEM-6 the dissociation degree was $\alpha_{IR} \leq 0.3$. From this we can learn that nearly all underlying COOH groups of the PAC were consumed by PEI and a newly adsorbed PAC provides again for new COOH groups to be dissociated by the next PEI layer.

For the PEM-5 of PDADMAC/PAC, not all COOH groups of the underlying PAC layer were consumed by PDADMAC (α_{IR}=0.70) and α_{IR} was significantly lower in the PEM-6 (α_{IR}=0.13). From this we can learn that in PDADMAC/PAC multilayers, fewer COOH groups are consumed than in PEI/PAC multilayers. This may be explained by the higher flexibility of PEI and the higher stiffness of PDADMAC. Since PAC at pH 4 should be in a coiled state, the stiffer PDADMAC might be not able to match all the carboxylic acid groups of PAC in a sufficient way, which is possible to a higher extent for the flexible PEI. PEMs of PDADMAC/PAC may therefore deviate more from 1:1 charge stoichiometry having higher uncompensated loop contributions, whereas PEMs of PEI/PAC are closer to 1:1 stoichiometry having fewer loops.

Similar relative results were found for the polyelectrolyte complexes: the α_{IR} of PEC-0.8 of PEI/PAC (0.4) was significantly higher than that of PEC-0.8 of PDADMAC/PAC. Also, according to Table 1, the α_{IR} of the PEC-0.80 was higher than that of the PEC-1.25 (0.20), which might be qualitatively analogous to the higher α_{IR} of the polycation terminated PEM-5 compared to PEM-6, respectively.

2.6.2 *Multilayers of PECs*

As a further surface modification, concept PEMs may be deposited using negatively and positively charged PECs. Recently, the consecutive adsorption of PEC^+ (n−/n+=0.6) of PDADMAC/PMA-MS with the respective PEC^- (n−/n+=1.6) was reported [94]. In contrast to oppositely charged polyelectrolytes, a lateral growth of the PECs was obtained, which was evident from ATR-FTIR spectral data. Obviously, the oppositely charged PEC nanoparti-

cles were growing laterally at the surface in contrast to the vertically growth of polyanions and polycations on top of eachother in PEMs from the 5th layer on, in which a homogeneous surface layer is established. These data illustrate that using spherical oppositely charged PECs, homogeneous polyelectrolyte layers can be built up. As it is previously shown (Fig. 6) this is not the case for uniquely charged ones (either PEC^+ or PEC^-) on oppositely charged surfaces, since there is a general jamming limit of adsorbing particles of about 55% as it is reported in [102]. However this surface modification concept might actually be too sophisticated at the moment for industrial applications and has to be simplified by experiment.

Furthermore, negatively charged PEC particles (PEC-1.6) of PLL and PMA-P can be consecutively adsorbed with PEI as the polycation to give homogeneous surface coverages, which is reported in [95].

2.6.2.1 Anisotropic Multilayers

A major challenge today is how to improve the orientation and the stability of the multilayers and how to characterize them properly.

Laschewsky et al., for example, formed organic-inorganic hybrid multilayers of polyelectrolytes and a clay that were stabilized by photocrosslinking [103]. Müller deposited cationic poly(L-lysine) (PLL) and polyanions like poly(maleic acid-*co*-α-methylstyrene) (PMA-MS) or poly(vinylsulfate) (PVS) by consecutively adsorbing on unidirectionally scratched silicon substrates [104]. The poly(L-lysine) formed α-helical rods in the multilayers that are aligned along the scratching direction of the substrate. He applied attenuated total reflection-Fourier transform spectroscopy (ATR-FTIR) using polarized light for the determination of the orientation within the films.

Representative dichroic ATR-FTIR spectra of consecutively adsorbed multilayers of PLL/PMA-MS in contact with an α-helix inducing 1m $NaClO_4$-solution are given in Fig. 8 for the untexturized substrate (A) and the texturized one (B). A significant variation of the relative amide I and amide II peak heights in the *p* and *s*-polarized ATR-FTIR spectra can be observed for the texturized substrate. From the dichroic ratios R of the amide I and amide II peak heights taken from the *p*-polarized and *s*-polarized spectra (i.e. $R_{\text{amide I}}=A_p(\text{amide I})/A_s(\text{amide I})$ and $R_{\text{amide II}}=A_p(\text{amide II})/A_s(\text{amide II})$), respectively, an order parameter S could be determined as it is described in [104]. Order parameters for α-helical PLL were found ranging from S=0.4 to 0.7 (S is equal to 1 for perfect orientation) in dependence of the chosen polyanion and parameters like the number of adsorption steps and the hydration state (dry/wet) of the sample. The degree of texturization and the molecular weight of PLL were found to be of main importance for the uniaxial alignment of the complexed α-helical rods [105]. Surfaces of anisotropically oriented α-helical polypeptides are interesting for biomimetic purposes. Further, oriented optically active rigid-rod polyelectrolytes [106] can become an essential building-block in nanosized electronic devices [107]. ATR-FTIR spectroscopy has proved itself to be very useful for a quantitative

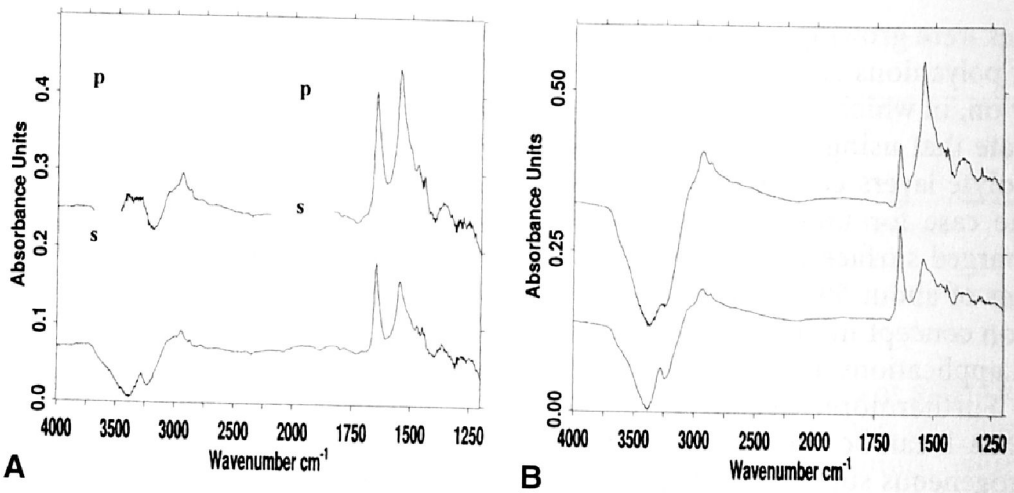

Fig. 8 *p*- and *s*-polarized in-situ-ATR-FTIR spectra of PLL/PMA-MS multilayers recorded after 10 deposition cycles on the untexturized (A) and on the uniaxially scratched Si substrate (B) in the presence of 1m $NaClO_4$ (wet state) in the range 4000-1200 cm^{-1}

in situ detection of the multilayer deposition and molecular changes within the multilayer phase induced by external stimulation [93]. Well investigated stimuli are the changing the pH [108], organic solvents [109], and humid air [93].

Concerning the latter, PEM composed of PEI and PMA-MS were described, which were deposited on silicon substrates and the water uptake from humid air (90% rel. hum.) of the dry sample was measured by ATR-IR spectroscopy. In Fig. 9, band areas of the ν(OH) band, which were normal-

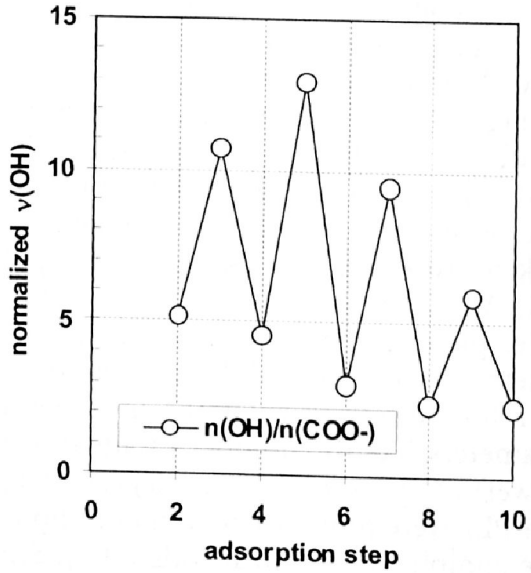

Fig. 9 Water uptake of the PEM-PEI/PMA-MS at 90% r.h in dependence of the adsorption step. The ν(OH) band area of difference spectra between hydrated and dry films was normalized by the $\nu(COO^-)$ at 1580 cm^{-1} (PMA-MS) to obtain a measure for thickness independent water uptake of the PEM

ized by the $\nu(COO^-)$ of the PMA-MS, are shown. By this normalization, the effect is compensated in that thicker layers absorb more water, so that the plotted data are a direct measure of thickness-independent water uptake. A modulated course of the water uptake can be observed in dependence on the adsorption step, whereby all polycation-terminated PEMs show a higher water uptake than that of the polyanion terminated ones. Moreover, wetting measurements (sessile drop) revealed a lower contact angle for the PEI-terminated PEM (43°) compared to the PMA-MS-terminated one (67°).

Similar results to these were found by Schwarz and Schönhoff [110] on nanoparticles coated by the PEM composed of poly(allylamine) (PAA) and PSS via ^1H NMR relaxation measurements. There, an increased water immobilization is reported for all odd polycation (PAA) terminating PEMs in contrast to even polyanion (PSS) terminating PEMs, which was found to be not just a property of the last adsorbed layer but more of the whole multilayer phase.

2.6.2.2 Protein/PEM Interaction

The possibility of a selective interaction between proteins and the outermost surface of polyelectrolyte multilayers [108] may become of outstanding importance in the development of engineering protein resistant surfaces for various biomedical applications by wet chemical surface modification.

As an example, results on the adsorption of human serum albumin (HSA) at a hydrophobic polypropylene (PP) film, which was modified by PEI/PAC multilayers are shown in Fig. 10 [111]. Based on ATR-FTIR spectra in the amide I region of the adsorbed protein layer the medium kinetic course

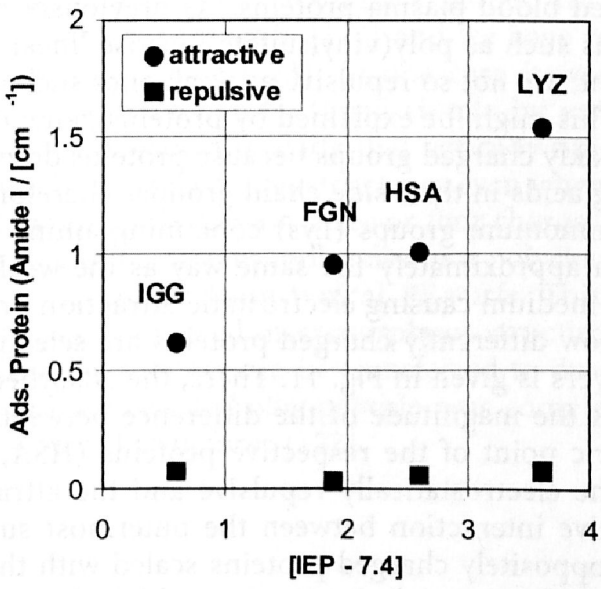

Fig. 10 Adsorbed amounts of the proteins HSA, FGN, IGG and LYZ at PAC (4) or PEI (5) terminating PEI/PAC multilayers in dependence of their IEP

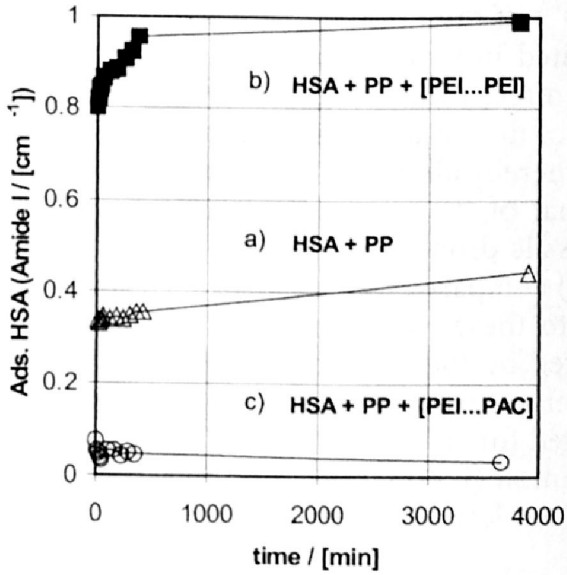

Fig. 11 Adsorbed HSA amounts on an unmodified and multilayer modified polypropylene (PP) film: (*a*) bare PP film, (*b*) CO_2-plasma treated PP-Film, modified by PEI (5) terminating PEM of PEI/PAC, (*c*) CO_2-plasma treated PP-Film, modified by PAC (4) terminating PEM

shows the moderate adsorption of HSA at the bare PP film, the lower the small adsorbed amount at the PP film modified by the polyanion capping multilayer and the upper course at the high adsorbed amount at the polycation terminating layer, respectively. Hence it is possible to modify hydrophobic polymer substrates by the PEM concept using commercial polyelectrolytes like PEI/PAC in order to control the protein affinity mainly by electrostatic interactions. In that framework especially weak polyanions are obviously very suitable to improve the protein resistance of surfaces towards negatively charged blood plasma proteins. As previously reported in [108], strong polyanions such as poly(vinylsulfate), whose linear charge density is not pH dependent, are not so repulsive as weak ones such as PAC, which are pH dependent. This might be explained by proteins being composed of amino acids with weakly charged groups because proteins do not contain amino acids with strong acids in their side chain groups. Therefore the carboxylate (Asp, Glu) or ammonium groups (Lys) containing amino acids of proteins are influenced in approximately the same way as the weak polyelectrolytes by the pH of the medium causing electrostatic attraction or repulsion.

An example how differently charged proteins are selectively adsorbed by PEI/PAC multilayers is given in Fig. 11. There, the adsorbed protein amount is plotted against the magnitude of the difference between the solution pH and the isoelectric point of the respective proteins (HSA, IGG, LYZ, FGN) [108] for both the electrostatically repulsive and the attractive case. Obviously the attractive interaction between the outermost surface of PEI/PAC multilayers and oppositely charged proteins scaled with the protein IEPs in contrast to the repulsive protein interaction, which showed no such dependence.

3
Polyelectrolyte-Surfactant Complexes (PE-surfs)

The complexation of polyelectrolyte with surfactants, which include numerous low and medium weight amphiphiles as well as lipids, has been investigated for many years nearly exclusively in solution as reviewed by Goddard [112]. Since 1994, starting with work by Antonietti et al. [15], polyelectrolyte-surfactant complexes (PE-surfs) in the solid state have also become of increasing interest. For some reviews see [1, 4-7, 113].

3.1
PE-Surfs in the Solid State

The most characteristic feature of solid-state PE-surfs is that they form a large number of mesomorphous structures which are liquid crystalline-like. These range from flat lamellar structures [114, 115] and discotic columnar structures [116] to periodic structures-*within*-structures [117]. The latter were first described by ten Brinke et al. [118]. The major factor that determines the type of the mesophase is the surfactant while the polyelectrolyte acts as a kind of glue between the charged surfactant head groups. Therefore, the polymer has normally the major influence on the mechanical properties of PE-surfs and not on the type of the mesophase [119]. But this is only a general rule. Chu et al. have shown that the charge density of the polyelectrolyte can also have a significant structural effect [120]. It has further been shown that the number of perforations increases in a perforated lamellar PE-surf system when the charge density of the polyelectrolyte increases [121].

In addition to the tuning of the structures, much attention is currently being paid to the physical properties. Tieke, for example, has produced mesomorphous photoluminescent PE-surfs [122] and we have reported PE-surfs that display electroluminescence [123]. In one case it was found that the electroluminescence spectrum can be tuned simply by varying the surfactant [124]. Faul et al. have shown recently that optically functionalized complexes can form highly organized nanostructures even when the polyelectrolyte is substituted by dyes that contain three or four charges [125, 126]. They show that the binding of surfactant molecules to a polycharged dye is a cooperative process as is known from typical PE-surfs. This proves that the concept of forming highly ordered mesomorphous structures from PE-surfs by a cooperative binding process can be transferred to dye-surfactant complexes. Similarly, GSSG, a charged oligopeptide, was complexed with surfactants to form well-ordered structures [127].

3.2
Dispersions and Nanoparticles

Three different ways have been developed to produce nanoparticle of PE-surfs. The most simple one is the mixing of polyelectrolytes and surfactants in non-stoichiometric quantities. An example for this is the complexation of poly(ethylene imine) with dodecanoic acid (PEI-C12) . It forms a solid-state complex that is water-insoluble when the number of complexable amino functions is equal to the number of carboxylic acid groups [128]. Its structure is smectic A-like. The same complex forms nanoparticles when the polymer is used in an excess of 50% [129]. The particles exhibit hydrodynamic diameters in the range of 80-150 nm, which depend on the preparation conditions, i.e., the particle formation is kinetically controlled. Each particle consists of a relatively compact core surrounded by a diffuse corona. PEI-C12 forms the core, while non-complexed PEI acts as a cationic-active dispersing agent. It was found that the nanoparticles show high zeta potentials (approximate to +40 mV) and are stable in NaCl solutions at concentrations of up to 0.3 mol l^{-1}. The stabilization of the nanoparticles results from a combination of ionic and steric contributions. A variation of the pH value was used to activate the dissolution of the particles.

The second way of forming nanoparticles of PE-surfs is to use water-soluble block-copolymers with one complexable (ionic) block and one non-complexable (nonionic) block. For example, the mesomorphous complexes (solid state) between poly(ethylene oxide)--b-poly(ethylene imine)s and dodecanoic acid can easily by dispersed in water to form nanoparticles [117]. The nanoparticles are of core-shell type and have sizes around 200 nm. Their cores are formed by poly(ethylene imine) dodecanoate while their shells consist of poly(ethylene oxide). It was found that the shapes of the nanoparticles depend on the PEI block. They are, for example, prolate if the PEI is linear and spherical if the PEI is branched.

A variation of this approach towards redispersible PE-surf nanoparticles was presented by Hentze et al. [130]. Their particle formation procedure is as follows: in a first step they prepared core-shell particles with a weakly cross-linked core of poly(styrene) and a shell of poly(ethylene oxide). Secondly, the cores were sulfonated to poly(styrene sulfonate). The cores were complexed with cationic surfactants in the third and final step. They became mesomorphous due to the complexation and show a characteristic length that varies between 2 and 4 nm depending on the alkyl chain length of the surfactant. The mean size of the whole particle is around 400 nm.

The third way to PE-surf nanoparticles is based on the use of polyampholytes, i.e. polyelectrolytes that contain cationic and anionic groups. Examples are long-term stable fluorinated nanoparticles, prepared by the complexation of polyampholytes with perfluorododecanoic acid [131]. The polyampholytes are statistic copolymers of styrylmethyl(trimethyl)ammonium chloride, methacrylic acid, and methyl methacrylate having more cationic monomers (28-100 mol %) than anionic monomers (0-16%). The cationic monomers form a complex with perfluorododecanoate ions to create neutral

entities that aggregate while the negatively charged methacrylic monomers prevent a macroscopic precipitation such as normally observed in fluorinated complexes. Negatively charged nanoparticles, which have zeta potentials of about −40 mV, are formed as a result of the combined complexation and stabilization. Small-angle X-ray scattering investigations reveal that the particles are anisotropic. For example, disk-shaped particles with a diameter of D greater than or equal to 30 nm and a height of 2.2 nm were formed for a high number of complexing groups (79 mol %). Cylindrical-shaped particles with lengths of H greater than or equal to 25 nm and radii of 1.5 nm were produced for a medium number of complexing groups (57 mol %). Fluorescence spectroscopy with pyrene as the probe was used to determine the critical aggregation concentrations of the particles which are in the range 0.01-0.06 g

The smallest known particles are prepared by using polyampholytes, that have short chain lengths, and with alternating cationic and anionic monomers along the polymer chain [132]. Fatty acids (dodecanoic acid and perfluorododecanoic acid) were used for complexation. The formation of the polyelectrolyte-fatty acid complexes is self-assembled and generates nanoparticles with sizes in the range of 3-5 nm that are named dressed micelles. A defined arrangement of the ionic charges of three polyampholytes was achieved by the copolymerization of a cationic vinyl monomer (*N,N'*-diallyl-*N'N*-dimethylammonium chloride) and anionic vinyl monomers (maleamic acid, phenylmaleamic acid, and 4-butylphenylmaleamic acid). The zeta potentials of the dressed micelles were adjusted in the range of −56 to 25 mV. They increase when replacing the alkylated dodecanoic acid by its perfluorinated counterpart, and they also increase when enhancing the hydrophilicity of the polyampholyte.

3.3 Drug Carriers

In addition to a better basic understanding of self-assembly processes one of the most attractive aims of the preparation nanoparticles of PE-surfs is the development of new drug delivery systems. These can be either simple drug carrier systems-or even more challenging-drug targeting systems. Promising candidates for drug carriers are complexes of poly(ethylene imine)s and fatty acids. They show loading capacities of hydrophobic drugs (e.g.,triiodothyronine and Q_{10}) in the range of 15 to 20% (w/w) [129].

Polyelectrolyte complexes of retinoic acid have been well investigated, they are pharmaceutically active surfactants. In the following, we will therefore discuss the physicochemical properties of drug carriers formed by synthetic polyamino acids, polyethyleneimine, double hydrophilic block copolymers and retinoic acid.

Vitamin A and its analogues, in particular retinoic acid, are involved in the proliferation and differentiation of epithelial tissues and have continued to be used in the treatment of dermatological disorders such as acne, psoriasis and hyperkeratosis [133, 134]. Currently, much effort is being focused on

how to understand the role of retinoic acid in cell differentiation. This is done by investigating the binding properties of retinoids on specific proteins [135] Their role in malignant-tumor inhibition [136, 137] and in their regulation of brain functions [138]. Natural retinoids need to be bound to specific retinoic-binding proteins in order to ensure their protection, solubility, and transport by body fluids. Immobilization is a major problem in administering retinoic acid as a pharmacological agent. One way of achieving such immobilization and protection of retinoic acid is by binding it to a protein as is the case in nature. A successful example for mimicking nature's strategy was shown by Zanotti et al. [139] when he cocrystallized transthyretin and retinoic acid. This, however, is a difficult and costly procedure. An easier and less expensive method for the required immobilization by the complexation of retinoic acid with synthetic cationic polyelectrolytes such as poly(ionene-6,3), poly(*N*-methyl-4-vinyl-pyridinium) and poly(diallyldimethylammonium) has been developed [140, 141].

The work presented in the next section concerns the immobilization of retinoic acid by three polyamino acids: poly(-L-lysine), poly(-L-arginine) and poly(-L-histidine). The mesomorphous structure of these complexes, which are prepared as nano-particles, has been examined. Then we will report on the physicochemical characteristics of water-soluble complexes formed between PEO-PLL block copolymers and retinoic acid. The structure in the solid-state and solution are discussed. Further the dissociation of the complex when changing the pH is reported. Finally, the immobilization of retinoic acid by PEI with different molecular weights is presented.

3.3.1
Immobilization of Retinoic Acid by Polyamino Acids [142]

The retinaote complexes of poly(L-arginine) (PLA), poly(L-histidine) (PLH) and poly(L-lysine) (PLL) were precipitated from aqueous solutions, purified and cast from solution in 2-butanol in order to form films. A drawing of the compounds used is shown in Fig. 12. In comparison to complexes of retinoic acid with other poly cations, such as poly(ionene-6,3), poly(*N*-methylene-4-vinylene-pyridinium) and poly(diallyldimethylammonium) [140], the dissolution rate of the polyamino acid complexes was significantly slower. In addition, films prepared from the former are flexible, have glass-transition temperatures in the range of -19 to 28 °C and show viscoelastic mechanical properties, whereas those of PLA, PLH and PLL are brittle. Differential scanning calorimetry showed no glass-transitions. The difference in the solubility and mechanical properties of retinoate complexes of polycations containing an atactic backbone and complexes with basic poly(L-amino) acids may be explained by the stereo-chemically unique polymer backbones of the latter, which enhance the stiffness of the retinoate complex. It has already been stated that no glass-transitions were found in solid-state complexes of poly(L-lysine) with alkyl sulfates [143] or soylecithin [144]. Therefore, at least for poly(L-lysine), the absence of a glass transition may be assumed to be a characteristic property of its solid-state complexes with surfactants.

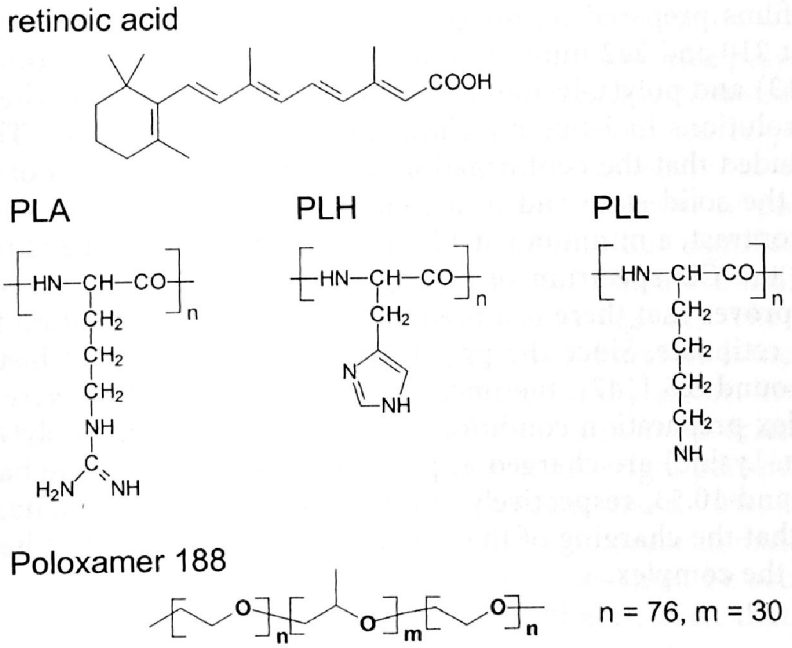

Fig. 12 Substances used for complex formation and nanoparticles. (retinoic acid) All-*trans* retinoic acid, (PLA) poly(-L-arginine), (PLH) poly(-L-histidine), (PLL) poly(-L-lysine). As dispersing agent a tri-block copolymer was used. It consisted of ethylene oxide and propylene oxide (Poloxamer 188). Reprinted with permission from [142]. Copyright 2000 American Chemical Society

3.3.1.1 Chain Conformation

The conformational state of the polymeric backbone of the complexes was examined by circular dichroism (CD). Figure 13 shows the CD spectra of

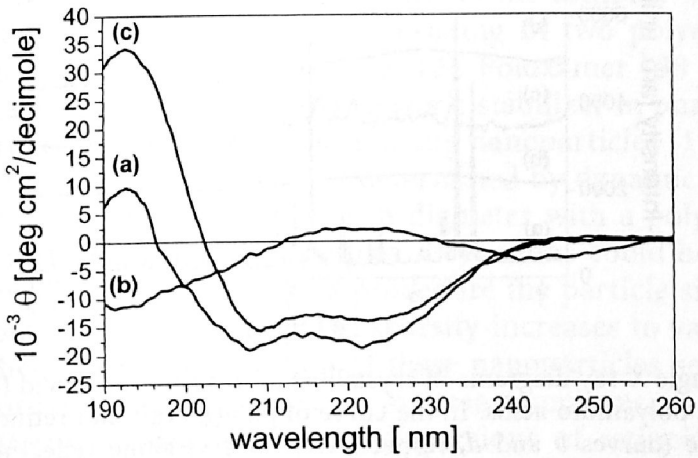

Fig. 13 Circular dichroism spectra of poly(L-arginine) retinoate (*a*), poly(L-histidine) retinoate (*b*), and poly(L-lysine) retinoate (*c*). The complexes were prepared as films on quartz slides. Reprinted with permission from [142]. Copyright 2000 American Chemical Society

complex films prepared on quartz slides. A maximum at 191 nm and two minima at 210 and 222 nm were found for poly(L-arginine) retinoate (curve a in Fig. 13) and poly(L-lysine) retinoate (curve c in Fig. 13). The spectra of complex solutions in 2-butanol show the same characteristics. Therefore, it was concluded that the conformation of the polymeric chains of both complexes in the solid state and in a solution of 2-butanol is an α-helix [145, 146]. By contrast, a minimum at 193 nm and a maximum at 222 nm was observed in the CD spectrum of poly(L-histidine) retinoate (curve b in Fig. 13). This proves that there is a predominantly coil conformation for poly(L-histidine) retinoate. Since the pK_a of the imidazole group of histidine residues is around 6.6 [147], the uncharged forms of histidine were present at the complex preparation condition (pH 9). By contrast the poly(L-arginine) and poly(L-Lysine) are charged at pH 9. The pK_a-values of the basic groups are 12.48 and 10.53, respectively [148]. On the basis of this data, it may be assumed that the charging of the polyamino acid leads to an α-helix conformation of the complex.

3.3.1.2 Solid-State Structures

Information about the molecular packing of the retinoate moieties was obtained by wide-angle X-ray scattering (WAXS). The WAXS pattern of retinoic acid (curve a in Fig. 14) is characterized by a number of sharp reflections resulting from the high degree of crystallinity. Retinoic acid crystallizes in two similar crystalline modifications (triclinic and monoclinic) [149], which produce the reflex pattern observed. As shown in Fig. 14, curves b and d,

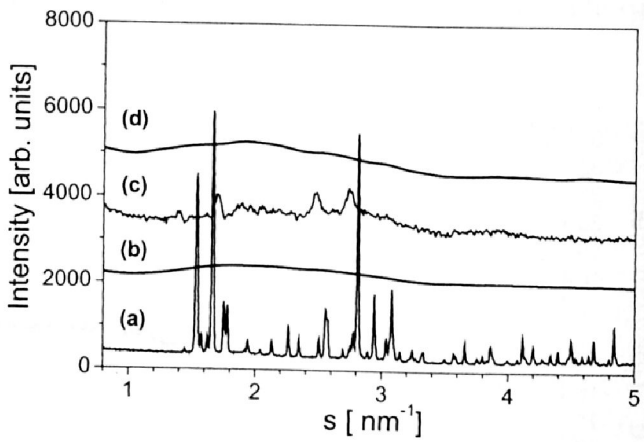

Fig. 14 Wide-angle X-ray diagrams of crystalline all-*trans* retinoic acid (curve *a*) and its complexes with polyamino acids. In the curve of poly(L-arginine) retinoate and poly(L-lysine) retinoate (curves *b* and *d*, respectively) no crystalline reflections were found. However, three weak crystalline reflections are present in the curve of poly(L-histidine) retinoate at s=1.69, 2.48 and 2.73 nm^{-1} (curve *c*). This is indicative of a partially crystalline complex structure. Reprinted with permission from [142]. Copyright 2000 American Chemical Society

the crystallinity of retinoic acid was prevented by complexation with poly(L-arginine) and poly(L-lysine). As is the case in complexes with polydiallylammonium chloride, ionene-3,6 and poly(*N*-methyl-4-vinylpyridinium chloride) [140], the maximum of the broad wide-angle reflection corresponds to a Bragg-spacing of 0.52 nm. The absence of sharp reflections in the wide-angle region proves the lack of crystallinity. Again, the properties of poly(L-histidine) retinoate differ from that of the others. Weak but significant reflections at s=1.69, 2.48 and 2.73 nm^{-1} were observed which are indicative for the partial crystallinity of the complex (curve c in Fig. 14). The scattering patterns remained constant for several months, and therefore it was assumed that the complexes are likely to be thermodynamically stable. The absence of crystallinity, is an interesting aspect, both from a material science as well as from a pharmaceutical point of view, because the weight percentage of the crystallizable retinoic molecules in all complexes is about 70%. The strong reduction of crystallinity was explained as follows: In order to maintain electrostatic neutrality, any diffusion of retinoic moieties must be accompanied by a correlated movement of charged polymer chains, such that no phase separation, and consequently no crystallization, can occur.

3.3.1.3 Nanoparticles

It was expected that the retinoate complexes of PLA, PLH and PLL form lamellar nanostructures similar to those reported earlier [140].The films of all complexes are optically anisotropic, as found during examination between crossed polarizers. Obviously the complexes are mesomorphous, but an unambiguous identification of the mesophases on the bases of the optical properties was not possible. Therefore, the state of order on a length scale of several nanometers was investigated by small-angle X-ray scattering measurements carried out on freeze-dried complex nano-dispersions. Aqueous nano-dispersions were prepared from powder of the complex with the aid of poloxamer 188, a triblock copolymer consisting of two polyethyleneoxide blocks and a polypropyleneoxide (see Fig. 12). Poloxamer 188 is a common non-ionic surfactant frequently used as a steric stabilizer in pharmaceuticals and already proved to be capable of stabilizing nanoparticles [150-152].

The size of the complex particles as determined by dynamic light scattering was in the range of 300 to 380 nm in diameter with a polydispersity of about 0.20. It was found that the complex dispersions could be redispersed after freeze-drying. As a result of this procedure the particle sizes increases slightly to about 400 nm and the polydispersity increases to values of about 0.3. The simplicity of the preparation of these nanoparticles seems to be an attractive feature of these complexes. As in these complexes, in the small-angle X-ray scattering diagrams of nano-dispersions of retinoate complexes equidistant reflections are also present (see Fig. 15). It can be seen that the positions and the sharpness of the scattering peaks are different for the complexes. In the case of poly(L-arginine) retinoate, a lamellar repeat unit of 3.62 nm was determined by fitting a Lorentzian peak profile onto the (001)

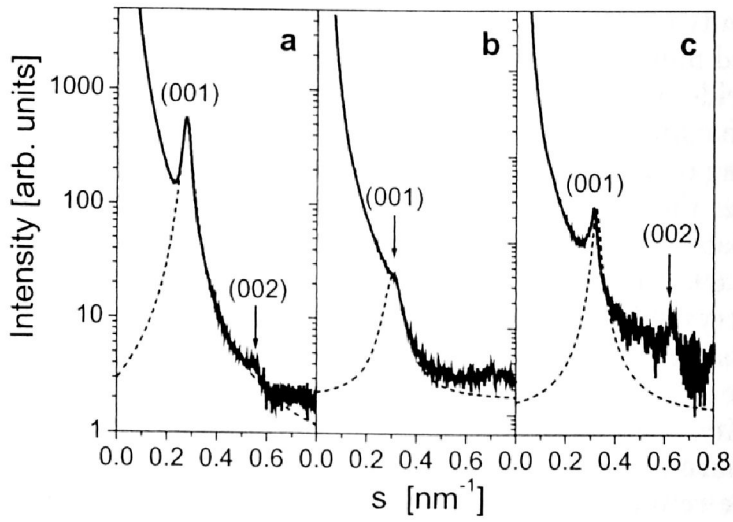

Fig. 15 Small-angle X-ray scattering curves of poly(L-arginine) retinoate (*a*), poly(L-histidine) retinoate (*b*) and poly(L-lysine) retinoate (*c*). The dashed lines are fits using a Lorentzian peak profile. Repeat units are 3.62 nm, 3.27 nm, and 3.10 nm. Reprinted with permission from [142]. Copyright 2000 American Chemical Society

reflection. The corresponding values for poly(L-histidine) and poly(L-lysine) are 3.27 nm and 3.10 nm, respectively. Obviously the size of the repeat unit increases with an increasing mass of the monomer. In addition, the increase of the size of the repeat unit is linear with respect to the mass of the monomer unit (+0.0185 nm per mass unit). This linear scaling is indicative of the smectic A-like structures of the three complexes.

The correlation lengths of the structures were determined from the reciprocal width of the reflections; they were 27±1, 15±3 and 38±1 nm (arginine, histidine and lysine). The correlation length values can be explained by an increasing stacking order of the smectic layers from poly(L-histidine) retinoate, poly(L-arginine) retinoate to poly(L-lysine) retinoate. Such differences may be the result of packing constraints due to their different molecular geometry, which may lead to different degrees of frustration [15]. The question arises as how to characterize the internal lamellar particle structure in detail. Parameters which are easily available are only the size of the particles and the size of the repeat units within them. In earlier works on polyelectrolyte surfactant complex films, it was found that a good model for the description of their mesophase structures could be made by the microphase separation of the ionic rich and hydrophobic rich regions. Often, the density transition between these regions is given by a step function, which is similar to that found for strongly segregated block copolymers and can be identified by the presence of Porod's law [182,183]. With such ideal phase-separated lamellar sheets within the complex nanoparticles, two limiting cases for their internal structures were assumed: an 'onion'-like and a 'tart'-like structure. As demonstrated earlier [142] it must be stated that currently the polydispersity (20%) of the complex nanoparticles is too large to produce de-

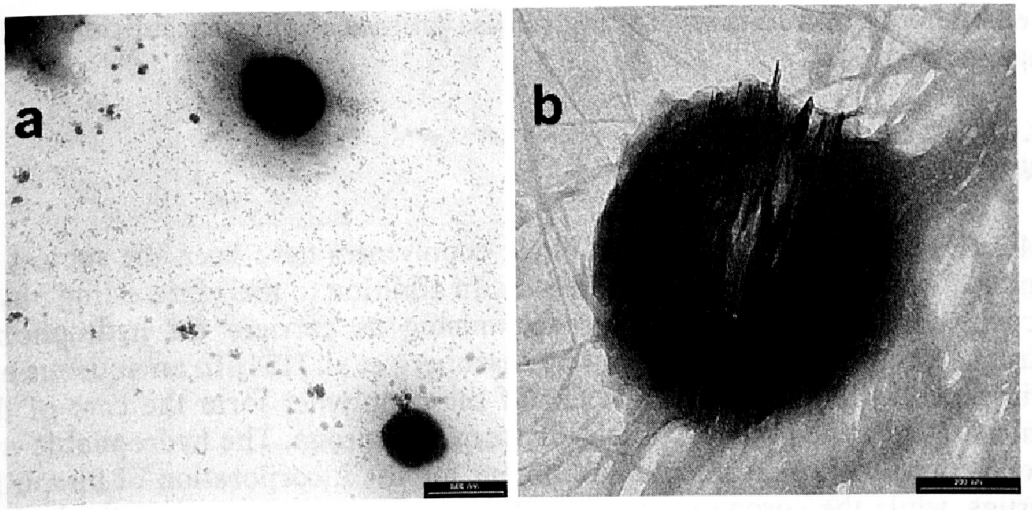

Fig. 16 Typical TEM pictures of a dried dispersion on a copper grid. (*a*) At lower resolution spherical complex particles are shown surrounded by a halo consisting of block copolymers (scale bar=500 nm). (*b*) At higher resolution, the internal structure of the particle is revealed to be tart-like (scale bar=200 nm). Reprinted with permission from [142]. Copyright 2000 American Chemical Society

tailed information about the nature of their internal structures such as onion- or tart-type by small-angle X-ray scattering.

For more insight into the internal particle structure, electron microscopy experiments were carried out. In TEM pictures of dried complex nano-particle dispersions (Fig. 16 a) it can be seen that the nanoparticles consist of a core with a high contrast, which is surrounded by a shell of lower contrast. It was believed that the core consists of the complex and the shell of the dispersing agent, Poloxamer 188. At a higher resolution (Fig. 16b) it can be seen that the internal structure of a dried particle is split into discrete layers, extending form one side of the particle to the other. This is very much indicative of a more tart-type particle structure. Therefore, on the basis of electron microscopy data it seems to be very likely that the kind of finite lamellar particle structure is much more of a tart-type than an onion-type [142]. As is the case in small-angle X-ray investigations currently being undertaken, it was not possible to determine the values of the lamellar thicknesses d_1 and d_2 by electron microscopy. The reason for the formation of the tart-type particles is not understood yet but may be due to their preparation from films. In films the lamellar domain size is likely to be much larger than the size of the nano-particles and tart-type.

In conclusion it was shown that the solid-state complexes formed by poly(L-arginine), poly(L-histidine) and poly(L-lysine) cations and retinoic acid can be prepared as films and nano-particles. The high content of retinoate moieties, the absence of crystallinity and low particle sizes could make these complexes interesting as a new carrier for the delivery of retinoic acid, either transdermal or in body fluids. It may be speculated that supramolecular structures such as the smectic A-like nano-particles of the tart-type pre-

sented here can lead to interesting release profiles of pharmaceutically active agents.

3.3.2
Block copolymers [153]

Micelles formed by amphiphilic block copolymers have been the subject of intense research during the last decade. In addition to their interesting physicochemical properties, they are promising as carriers for hydrophobic drugs. A recent review was given by Eisenberg et al. [154] In an aqueous environment, the hydrophobic blocks of the copolymer form the core of the micelle while the hydrophilic blocks form the corona. The hydrophobic micelle core serves as a microenvironment for the incorporation of lipophilic drugs, while the corona serves as a stabilizing interface between the hydrophobic core and the external medium. It was shown that complexation of poly(ethylene oxide)-*b*-poly(L-lysine)s (PEO-PLL) with DNA as an oppositely charged polyelectrolyte leads to the formation of water-soluble complexes in an aqueous environment [155]. PEO-PLL block copolymer micelles were used to explore the feasibility of polymeric micelles as a novel vector system for genes and oligonucleotides [156, 157]. Supramolecular association of a block copolymer consisting of PEO and polyamino acids through hydrophobic or electrostatic interaction leads to the formation of core-shell type micelles in which drug molecules are hydrophobically or electrostatically included in the core of the particle which is surrounded by the PEO outer shell [158]. The proper micelle size of about 50 nm and the hydrophilicity of the outer-shell PEO seem to contribute to an extension of the period for which the drug circulates in the blood. Exceptionally high accumulations in a solid tumor were demonstrated for copolymer micelles with an entrapped anticancer drug (doxorubicin) [159, 160]. Kabanov et al. proposed a similar system, the complex of poly(ethylene oxide)-*g*-polyethyleneimine and biological active surfactants, as a novel drug delivery system [161]. Such complexes form 'micellar microcontainers' with retinoic acid, a molecule which is highly optically active and is considered to be a surfactant from the physicochemical point of view. In the previous chapter it was shown that nanoparticles of complexes of synthetic polyamino acids with retinoic acid contain an internal smectic A-like structure.

This section reports on the physicochemical characteristics of water-soluble complexes formed between PEO-PLL block copolymers and retinoic acid. Two block copolymers were used. The lengths of the PEO blocks in both are identical, the molecular weight was 5000 g/mol (M_w/M_n=1.1). This corresponds to a degree of polymerization of 114. The length of the PLL block varies: PEO-PLL18 has 18 L-lysine monomer units and PEO-PLL30 has 30. A sketch of the molecular structures is given in Fig. 17.

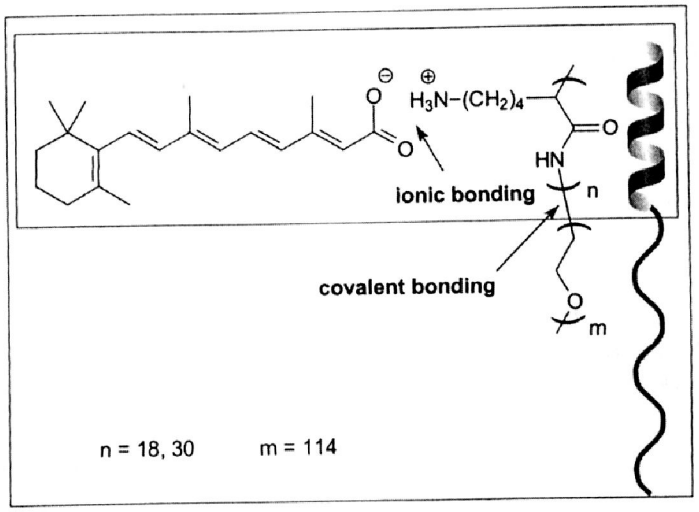

Fig. 17 The molecular structure of *a* poly(ethylene oxide)-*b*-poly(L-lysine) retinoate complex and a sketch of the polymeric backbone with an α-helical poly(L-lysine) block. Reprinted with permission from [153]. Copyright 2000 American Chemical Society

3.3.2.1 Crystallinity

DSC traces of the copolymers and of their complexes with retinoic acid in the solid state showed that the two non-complexed polymers undergo first-order transitions upon heating with a maximum at 56±1 °C. Upon cooling the transitions were found at 35±2 °C. The DSC traces of the complexes differ significantly from those of the polymers. A weaker transition is present in the curve of PEO-PLL18 retinoate at 47 °C when it is heated and at 23 °C when it is cooled. In the DSC curves of PEO-PLL30 retinoate, a very weak transition at 38 °C was detected on heating, while it was not found during cooling. No other transitions were observed in the temperature range of 0 to 150 °C. Homopolymers of poly(ethylene oxide) are known to form lamellar crystals with melt transitions that depend significantly on their molecular weights. As an example, the melting points of poly(ethylene oxide)s with narrow molecular weight distributions are found at 48, 58 and 64 °C for molecular weights of 1500, 3000 and 6000 g/mol respectively [162]. Earlier no melt transition had been found for the complex of a homopolymer of poly(L-lysine) and retinoic acid and the melting point of retinoic acid is 181 °C [163]. Therefore, the transitions in the copolymers and in their complexes were regarded as due to the melting of the crystalline poly(ethylene oxide) segments. Compared to a poly(ethylene oxide) homopolymer with a molecular weight of 5000 g/mol, its co-polymerization with a poly(L-lysine) block lowers the melting transition of poly(ethylene oxide) by about 5 °C. Here the melting point depression does not depend on the length of the lysine block. For the complexes the lowering of the melt transition temperature is much stronger and depends on the length of the lysine block (17 °C and 26 °C for PEO-PLL18 retinoate and PEO-PLL30 retinoate, respectively). The measured

enthalpies of the melt transitions were compared with the perfect heat of fusion of PEO (203 J/g) [164] in order to estimate the degree of the bulk crystallinity. Taking into account the different amount of PEO in the compounds, the crystallinity of the PEO chains was found to be about 50% (PEO-PLL18), 45% (PEO-PLL30), 30% (PEO-PLL18 retinoate) and 10% (PEO-PLL30 retinoate). Compared to neat PEO whose crystallinity is in the range of 70 to 80% [164], the copolymerization with lysine reduces the degree of crystallinity by 20 to 30%. This is similar to the effect of blending PEO with PMMA [164]. In contrast to the copolymerization, the complexation reduces the degree of crystalline PEO even more strongly. Probably the complexed moieties disturb the formation of the extended chain conformation and the integral number of folded chain conformations, which are typical for the crystalline form of PEO [165]. The conclusion that crystalline PEO segments are the origin of the endothermic transitions was confirmed by wide-angle X-ray experiments. It was found that the X-ray scattering intensities of the PEO reflections at scattering vectors of s=2.18 nm^{-1} and 2.65 nm^{-1} decrease in the series PEO-PLL18, PEO-PLL30, PEO-PLL18 retinoate and PEO-PLL30 retinoate. This sequence of the intensities is in agreement with a decreasing amount of crystalline PEO segments in the samples derived by DSC.

3.3.2.2 Nanostructures in the Solid State

Small-angle X-ray scattering techniques were used to investigate the structure of the PEO-PLL polymers and their complexes on length scales in the range of 1 to 50 nm. The small-angle scattering diagrams of the PEO-PLL18 and PEO-PLL30 are essentially identical and show two Bragg peaks whose positions have a ratio of $1:3^{1/2}$ (not shown). This suggests a hexagonal arrangement of the poly(L-lysine) chains in a two-dimensional lattice with a center-to-center distance of 1.53 nm. This value is close to the chain spacing in poly(L-lysine) hydrochloride crystals (1.50 nm) [166]. In contrast to the pristine polymers, Bragg peaks with relative positions of 1:2 were found in the small-angle scattering diagrams of PEO-PLL18 retinoate and PEO-PLL30 retinoate, which indicate lamellar structures (see Fig. 18a,b). The long periods are 3.37 nm±0.05 nm (PEO-PLL18 retinoate) and 3.32 nm±0.05 nm (PEO-PLL30 retinoate), which is slightly larger than that found for a complex of a poly(L-lysine) homopolymer (M_v=15,000 to 30,000 g/mol) and retinoate, which is 3.10 nm [142]. This was attributed to a better packing of the latter as a result of the absence of packing constraints caused by PEO blocks. It can be seen in the scattering diagrams that the peaks of the PEO-PLL18 retinoate are broader than that of the PEO-PLL30 retinoate. The correlation lengths were 10 nm and 12 nm as determined from the width of the first order reflection. When taking into account the relative shortness of the lysine chains, the high degree of mesomorphous ordering is surprising.

Well defined conformations of the poly(L-lysine) chains have to be taken into account. It was found that in the solid state form of the non-complexed polymers, the poly(L-lysine) chains adopt mixtures of α-helix and β-sheet

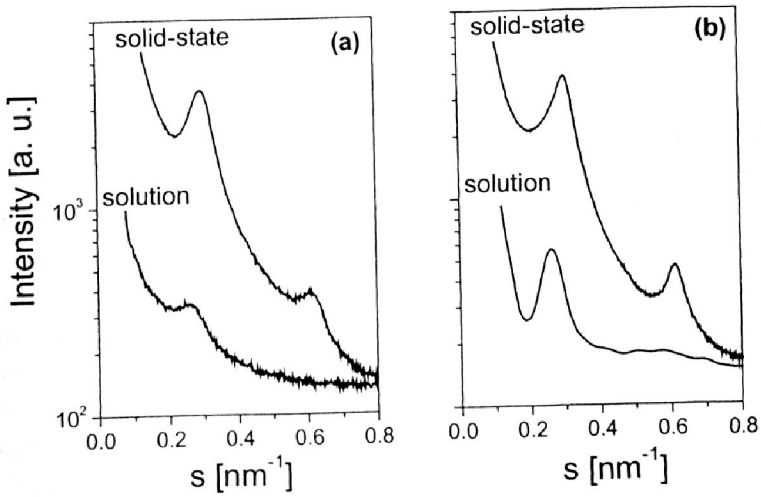

Fig. 18 Small-angle X-ray scattering curves of PEO-PLL18 retinoate (**a**) and PEO-PLL30 retinoate (**b**). Curves are given for the materials in the solid state (*upper curves*) and for dispersion in aqueous solution (*lower curves*). Reprinted with permission from [153]. Copyright 2000 American Chemical Society

conformations as shown by the position of the amide I and amide II vibrations in the FTIR spectrum [167] (see Fig. 19). It can be seen that the amide I vibrations of the α-helix is represented with a band at 1652 cm^{-1} and that of the β-sheet with a band at 1624 cm^{-1}. The individual amide II vibration bands overlap but the band at 1539 cm^{-1} is strongly indicative of significant amounts of β-sheet conformations. It was found that the intensity of the bands and consequently the amount of α-helix and β-sheet conformations depend to a significant degree on the preparation conditions such as solvent, temperature and drying time. Therefore it was not possible to identify differences in the conformations between PEO-PLL18 and PEO-PLL30. In contrast to the non-complexed polymers the positions of the amide I and amide

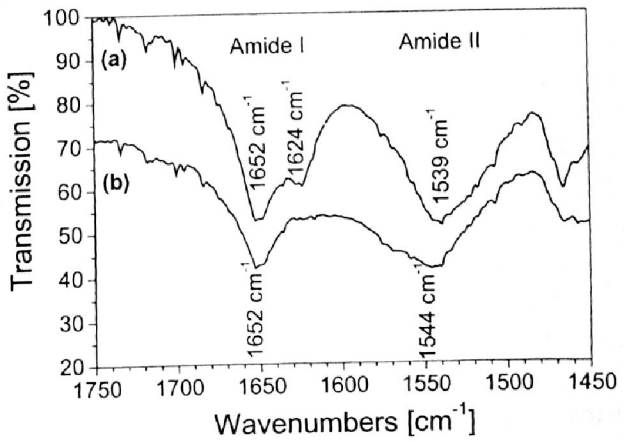

Fig. 19 FTIR spectra of the PEO-PLL18 (*a*) and the PEO-PLL30 retinoate (*b*) in the amide region. Reprinted with permission from [153]. Copyright 2000 American Chemical Society

II bands were found to be independent of the preparation conditions at 1652 cm^{-1} and 1544 cm^{-1} for PEO-PLL18 retinoate and PEO-PLL30 retinoate (Fig. 19b). This proves that the poly(L-lysine) chains strictly adopt an α-helix in the complexes. It was suggested that the α-helix in the PEO-PLL retinoate complexes is energetically more stable than the β-sheet conformation, which is probably due to a better spherical arrangement of the retinoate moieties when bound to an α-helix. Tirrell et al. reported on the structure of poly(L-lysine) complexes with alkyl sulfates which form lamellar structures [168]. They found that the α-helical and β-sheet portions of the poly(L-lysine) chains in their complexes depend to a great extent on the conditions of the preparation of the solid-state complexes from solution. The exact reason for the adjustment of the different chain conformation is not clear yet, but it was assumed that the formation of inter chain hydrogen bridges, which favors the β-sheet formation, is strongly suppressed for the two PEO-PLL retinoate complexes but not for the complexes of poly(-L-lysine) with alkyl sulfates.

3.3.2.3 Core-Shell Nanoparticles

Block copolymers containing a PEO block as a water-soluble segment and a second, water insoluble block, are known to be suitable for the formation of core-shell micelles, where the cores can be loaded with hydrophobic drugs [154]. Following this hydrophilic-hydrophobic concept the double hydrophilic PEO-PLL18 and PEO-PLL30 block copolymers were converted into hydrophilic-hydrophobic systems by their complexation with retinoic acid, which resulted in micellar solutions of the complexes. The solutions were investigated by X-ray scattering in an aqueous medium in the concentration range of 0.5 to 5% (w/w). The absence of reflections in the wide-angle scattering diagrams proved that no crystalline retinoic acid was formed during the complexation and that the PEO blocks are dissolved. In contrast to the wide-angle region sharp reflections were found in the small-angle diagrams of the micelles (see Fig. 15a,b) with Bragg spacings of 3.94 nm (PEO-PLL18 retinoate) and 3.83 nm (PEO-PLL30 retinoate). This was interpreted as resulting from mesomorphous core-shell micelles. The core which contain the PLL-retinoate moieties is of a lamellar structure and the shell is formed by PEO segments. The higher long period in the micelles compared to those of the complexes in the bulk material was explained by the incorporation of water in the core. From the differences of the long periods between the solid state complexes and the dispersed complexes the water content of the cores was estimated to be 17% (v/v) for PEO-PLL18 retinoate and 15% (v/v) for PEO-PLL30 retinoate. These values are close to the water uptake (18%) of a polyelectrolyte fluorosurfactant complex, in which the water is predominantly located around the polymeric backbone [169]. The location of the incorporated water and its mobilizing effect on the molecular dynamics is given in a detailed solid-state NMR investigation on polyelectrolyte-surfactant complexes [170].

From the widths of the reflections of the micellar solutions (Fig. 18) the correlation lengths of the mesophases within the cores were determined to be 6 nm (PEO-PLL18 retinoate) and 10 nm (PEO-PLL30 retinoate). It is known that, in a helical poly(amino acid), the amino acid monomer expands over 0.15 nm [171, 172]. In the case of poly(L-lysine)s (the polymerization degree of lysine is 18 and 30) the helical end-to-end distances were calculated to be 2.7 nm and 4.5 nm. Tentatively an α-helical conformation was assumed for the complexed PLL in the core of the micelles, the maximum lamellae stack size is about the same magnitude as the correlation lengths. Therefore it is probable that each micellar core contains a lamellar monodomain. Ten Brinke et al. have shown that a hierarchy of two different length scales (4.8 nm and 35.0 nm) can be produced when combining covalent bonding (block copolymer)s, proton transfer and hydrogen bonding [173]. PEO-PLL18 retinoate and PEO-PLL30 retinoate in the solid state could be considered to be similar to their block copolymer complexes. But in addition to the lamellar structuring of the PLL retinoate a regular structure with a larger long period (10 to 50 nm) could not be identified, which would have been expected from a microphase separation of PEO and PLL retinoate.

3.3.2.4 Helix-Coil Transition

A detailed investigation of the helix-coil transition of the non-complexed PEO-PLL18 has been reported on by Kataoka et. al [145]. By using circular dichroism they have shown that the PLL blocks of PEO-PLL18, which themselves cannot form an α-helix structure due to substantially lower molecular weight, form an α-helix structure in solution when they are bound to PEO. Their work shows clearly that the copolymerization with PEO has a stabilizing effect on the α-helical conformation of PLL. Bearing this in mind it was asked how the complexation of the PEO-PLL polymers affect the conformation of the PLL blocks. Circular dichroism was used as a sensitive method for the detection of the PLL chain conformations within the micelles. It was found that the shape of the circular dichroism spectra were neither dependent on the concentration of the complexes in a concentration range of 0.05 to 0.5% (w/w) nor does it depend on the storage time after preparation (1 h, 24 h, 72 h). In addition the spectra of PEO-PLL18 retinoate and PEO-PLL30 retinoate are identical within the range of experimental error. But, as expected, the spectra change with the variation of the pH value. This is shown in Fig. 20. It can be seen that a right handed α-helix structure, which is characterized by a maximum at 191 nm and two minima at 210 and 222 nm, is present at pH 9. A sketch of the polymer conformation is given in Fig. 17. The circular dichroism spectra change gradually when lowering the pH and adopt the form of a random coil at pH 3.7, the spectrum of these is characterized by a minimum at about 201 nm and a maximum at about 220 nm. The crossover wavelength remained at 204 nm. It should be noted that this crossover wavelength agreed well with that of the pH-induced helix-coil transition for poly(L-lysine) and PEO-PLL reported in the literature [145,

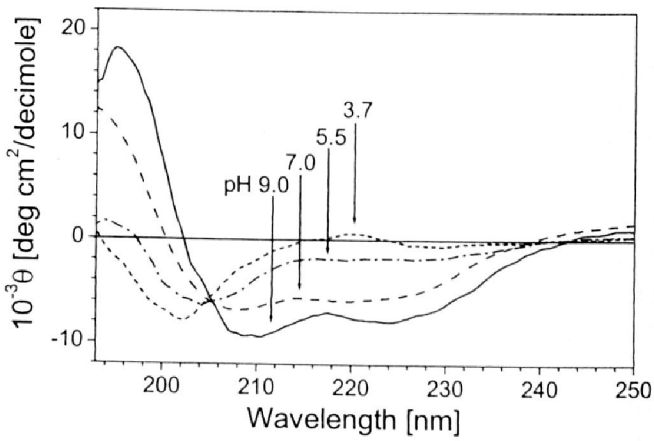

Fig. 20 Circular dichroism spectra of PEO-PLL18 retinoate as a function of the pH value. Reprinted with permission from [153]. Copyright 2000 American Chemical Society

174, 175]. Contributions of β-sheet structures to the spectra were not found to be present. It was concluded that the PLL conformation in the PEO-PLL18 retinoate and PEO-PLL30 retinoate micelles adopts an α-helix for pH values higher than 9.0 and a random coil at a pH lower than 3.7, while between these limiting values a mixture of α-helical and random coil structures is present.

According to Greenfield and Fasman [175], the content of α-helices was estimated from the mean molar ellipticity at a wavelength of 222 nm. It can be seen in Fig. 21 that the α-helix content decreases gradually in the range from pH 9 (95%) to pH 7 (70%). This is followed by a steep decrease occurring between pH 7 and pH 5, from 70 to 20% and approaches zero at about pH 3.7. The stability of the α-helix within the complexes is remarkable when bearing in mind that the helix-coil transition of poly(L-lysine) homopolymers is found at pH 10.3 and 25 °C where the polymer is 35% charged [176].

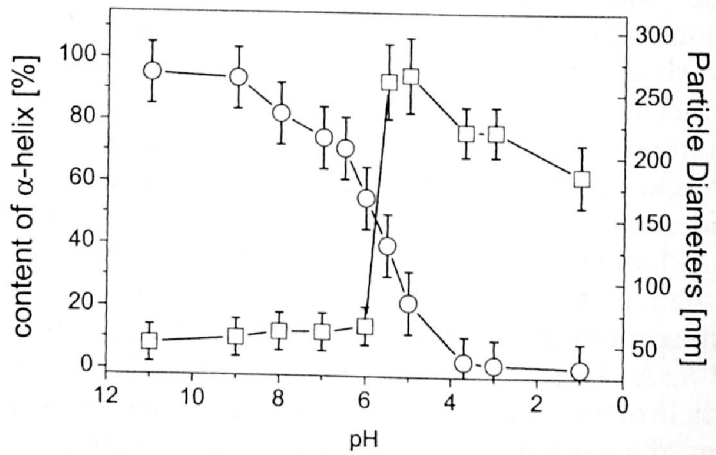

Fig. 21 Variation of the content of the complex in an α-helical state (*circles*) and the particle diameters of the PEO-PLL18 retinoate (*squares*) depend on the pH value. Reprinted with permission from [153]. Copyright 2000 American Chemical Society

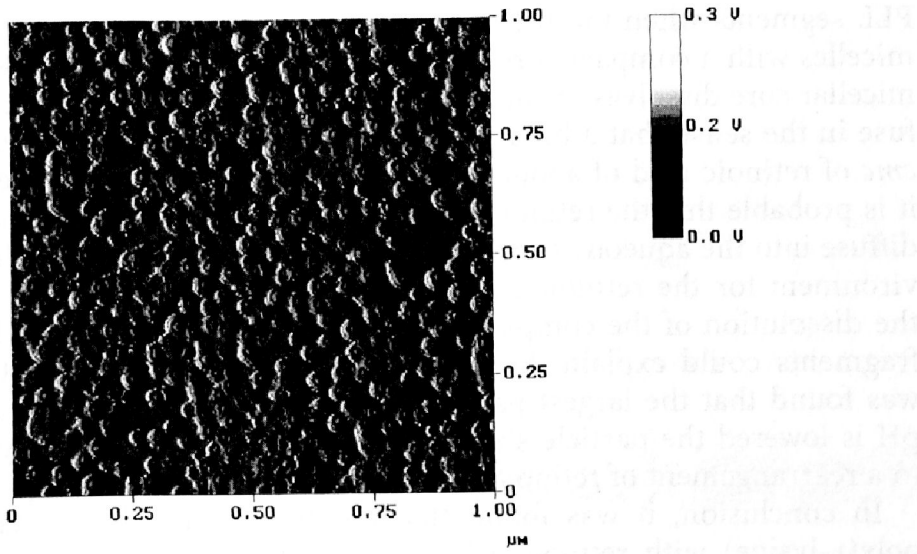

Fig. 22 AFM amplitude picture of a PEO-PLL30 retinoate dispersion (pH 9) dried on mica. Reprinted with permission from [153]. Copyright 2000 American Chemical Society

It was assumed that the α-helix of the complexes is stabilized, firstly by the PEO corona, and secondly by protecting retinoate molecules. This process ends when the retinoate moieties become protonated. This assumption is supported by the pK_a of retinoic acid which is in the range of 6 to 8 and depends strongly on its surroundings, concentration and microenvironment [177, 178]. In order to characterize the size of the micelles, samples of micellar solutions were stored and analyzed by dynamic light scattering directly after the circular dichroism measurement. It was found that the mean particle size was dependent on the pH value. The particle sizes of PEO-PLL18 retinoate and PEO-PLL30 retinoate are essentially the same. At a high pH, where the α-helical conformation of the PLL is predominant and where the retinoic acid has a deprotonated form, the smallest particle sizes are observed. In the range form pH 11 to pH 6 the mean particle diameter increases slightly from 50 nm to 60 nm. Then at pH 5.5 the mean diameter increases to values higher than 250 nm and it decreases constantly down to values of about 180 nm at a pH of 1.

The pH dependency of the particle sizes was confirmed by AFM measurements. An example of PEO-PLL30 retinoate at pH 9 is shown in Fig. 22. The core-shell morphology leads to significantly different AFM amplitudes at the center of the micelles than those in their corona. Exact measurements of the core diameters are not possible on the basis of the AFM data due to the softness of the PEO but the micellar sizes are relatively uniform and agree essentially with the correlation lengths determined by small-angle X-ray scattering. It is interesting that the particle sizes increase considerably within a small range of variation of the pH, namely from 6.0 to 5.5. This is exactly in the region where the content of α-helical conformation decreases most rapidly. The interpretation is that the retinoic acid is bound ionically to the

PLL segments when the pH is higher than 6. This leads to small core-shell micelles with a compact core. At a pH of 5.5 the ionic bonds are broken, the micellar core dissolves or the distinct core-shell structure becomes more diffuse in the sense that a broad core-shell transition develops. Due to the low *cmc* of retinoic acid of about 2×10^{-6} mol/L (pH 7) in aqueous environment, it is probable that the retinoic acid clusters within the micelles and does not diffuse into the aqueous surroundings. The micelle is the most lipophilic environment for the retinoic acid in its protonated form. On the other hand, the dissolution of the compact micellar core into a number of hydrophobic fragments could explain the considerable increase in the particle sizes. It was found that the largest particle sizes are found around pH 5. When the pH is lowered the particle sizes decrease significantly. This is probably due to a rearrangement of retinoic acid clusters due to the lowering of the pH.

In conclusion, it was found that complexes of poly(ethylene oxide)-*b*-poly(L-lysine) with retinoic acid with short poly(L-lysine) segments of 18 and 30 monomers form core shell micelles. The cores of the micelles contain a lamellar smectic A-like structure, formed by a poly(L-lysine) retinoate complex, which is surrounded by a corona of poly(ethylene oxide). Although the poly(L-lysine) chains are relatively short, they adopt an α-helical conformation to a pH as low as 9. This effective stabilization of the α-helix structure seems to be due to the formation of a protective surrounding coat of retinoate and a shell of poly(ethylene oxide).

3.3.3
Polyethyleneimine [179]

The immobilization of retinoic acid by branched PEI with different molecular weights (6 10^2 to 2×10^6 g/mol) is described in the following section. The main interest is on the formation of mesomorphous structures, the release of retinoic acid from its complexes and the formation of nanoparticles.

3.3.3.1
Nanostructures

The optical micrographs of the PEI-retinoate complexes observed between crossed polarizers show that all complexes are highly birefringent, with textures that are independent of their molecular weights [179]. Similar textures are known for some lyotropic lamellar systems of phospholipids [180]. They originate from bilayers that were initially horizontal and corrugate in one or two dimensions to form domes and basins, and each appears as a 'Maltese cross'. In contrast, typical textures of elongated crystals are found in the micrograph of non-complexed all-*trans*-retinoic acid when it is prepared in the same way as the complexes. It was found that a ratio of amino functions to carboxylic acid groups of about 2:1, or higher, is necessary to prevent the crystallization of parts of the retinoic acid. This finding is in agreement with earlier studies in which it was reported that only the primary and the sec-

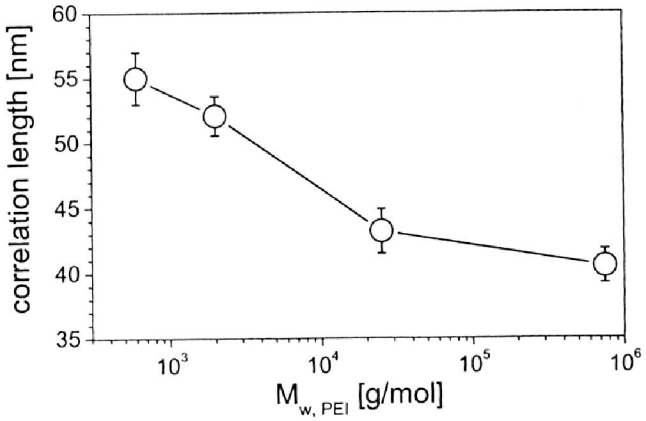

Fig. 23 The correlation length of the lamellar mesophase of the PEI-retinoate complexes depending on the molecular weight of the PEI. Reprinted with permission from [179]. Copyright 2000 American Chemical Society

ondary amino functions could be complexed by surfactants but not the tertiary groups [181]. The amount of the tertiary groups is around 25% in the PEIs used for complexation. This explains why an excess of amino functions, with respect to the carboxylic acid groups, has to be achieved for a complete complexation of the retinoic acid and to avoid crystallinity. Small-angle X-ray scattering measurements, which were carried out on films with thicknesses in the range of 0.05 mm to 1 mm, were used for a quantitative comparison of the complexes. An intense Bragg reflection was found in the scattering curves of all complexes at a scattering vector of about 0.3 nm^{-1}. The shapes of the curves were independent of the thicknesses of the films but they vary with the molecular weight of the PEI. Although no higher order reflections were observed for the complexes in the bulk material, together with the results from polarization microscopy and the fact that in earlier studies only lamellar structured complexes of retinoic acid were found [140] a lamellar structured mesophase for the PEI-retinoate complexes was proposed This assumption will be confirmed later in the section on thin films. The lamellar spacings increase slightly with the increasing molecular weight of the PEI and were determined to be 3.3 nm (PEI-600), 3.4 nm (PEI-2000), 3.4 nm (PEI-25000), and 3.5 nm (PEI-750000). This indicates higher ordered structures of the complexes with the lower molecular weight PEIs than the complexes with higher molecular weight PEIs.

The correlation lengths of the complexes, which were determined from the widths of the reflections, decrease with increasing molecular weight, from about 55 nm to 41 nm (see Fig. 23). This is a further indication for a higher order of the complexes with the PEI of low molecular weight. A probable reason for this influence of the molecular weight PEI on the supramolecular order is that a higher molecular weight would lead to higher packing constraints than a lower molecular weight would do. In addition to the reduction of the order of the lamellar structures this may lead to different degrees of frustrations [15]. The relations between the order and release profiles of retinoic acid from the complex films will be discussed later. In

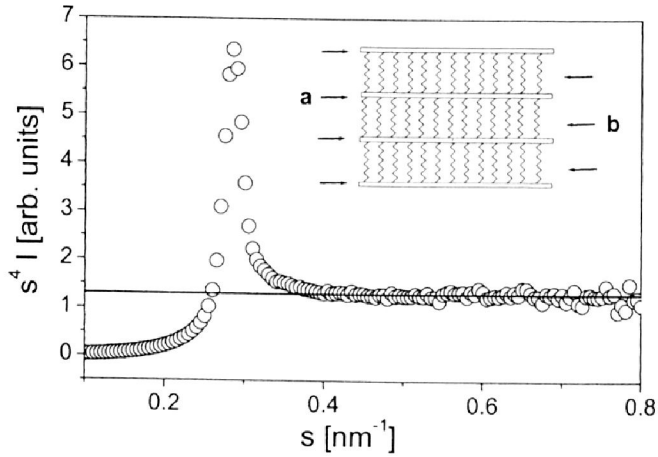

Fig. 24 Small-angle X-ray scattering intensity in a $s^4I(s)$-s-plot (*circles*). The *solid line* represents the best fit according to Porod's law at scattering vectors in the range of 0.4 to 0.8 nm^{-1}. The *insert* shows an idealized model of smectic A-like PEI retinoate structures, consisting of well-separated supramolecular lamellar sheets: (*a*) ionic layers with thicknesses of 0.6 nm (PEI-600), 0.7 nm (PEI-2000 and PEI-25000) and 0.8 nm (PEI 750000); (*b*) nonionic layers with thicknesses of 2.7 nm (PEI-600, PEI-2000, PEI-25000 and PEI-750000). Reprinted with permission from [179]. Copyright 2000 American Chemical Society

earlier works on polyelectrolyte surfactant complexes it was found that a good model for the description of their mesophase structures could be made by placing the microphase separation into ionic and hydrophobic regions. Often the density transition between these regions is sharp and is similar to that found for strongly segregated block copolymers. Sharp phase boundaries are identified by the application of Porod's law [182, 183]. The values of $s^4I(s)$, as shown in Fig. 24, were found to be constant for a scattering vector in the range of 0.4 to 0.8 nm^{-1}. This proves that the structures of the complexes are consistent with Porod's law. A broader transition or a statistical structuring of the domain boundary, as typically observed in microphase-separated block copolymers [182], can be excluded. Small deviations from a sharp boundary would indicate a significant deviation from Porod's law [183]. Therefore it was concluded that the phase boundaries of the complexes are of the order of 1 to 2 atomic distances. Using Eq. (1.2) in Ref [1], the average chord lengths were calculated to be 0.93 nm (PEI-600), 1.06 nm (PEI-2000), 1.10 nm (PEI-25000), and 1.22 nm (PEI-750000). These values are similar to the polymeric complexes of siloxane surfactants investigated earlier [184]. The simplest complex structure, which is in agreement with these numbers is a microphase-separated model constructed from a smaller ionic phase (polyelectrolyte plus ionic head groups) and a larger nonionic phase (hydrophobic moieties). The slight increase of l_p with the increasing molecular weight of the PEI is consistent with the assumption that the packing of the structure of the complexes is better for the low molecular weight complexes than for the high molecular weight complexes. The thicknesses d_1 and d_2 of the lamellae within the smectic A-like structures of the complexes were calculated using Eq. (1.12) in Ref [1]. The values are d_1=0.6

nm, d_2=2.7 nm (PEI-600), d_1=0.7 nm, d_2=2.7 nm (PEI-2000), d_1=0.7 nm, d_2=2.7 nm (PEI-25000) and d_1=0.8 nm, d_2=2.7 nm (PEI-750000). d_1 was assigned to the ionic lamellae, which are enriched in the polyelectrolytes plus the carboxylic head groups, and d_2 to the nonionic lamellae, which are enriched in the retinoic acid tails. As expected, the value of d_1 increases slightly with the molecular weight of the PEI, while the value of d_2 do not depend on the weight of the PEI used for complexation. A sketch of the structure is given in Fig. 24 (insert).

3.3.3.2 Thin Films

Thin films of the complexes on silicon wafers were prepared by the spin-coat technique from solutions of the complexes. The film structures were investigated by X-ray reflectivity. Reflectivity curves of thin films are shown in Fig. 25. Similarly to complexes of a fluorinated surfactant [1], well-defined double-layer stacks developed within a few seconds simply as a result of the deposition of droplets of the solutions of the complex. The molecular weight of the PEI increases in the line from curve a to d. The presence of Kiessig fringes in curves a and b indicate smooth films for the complexes PEI-600-retinoate and PEI-2000-retinoate. No Kiessig fringes were observed for the complexes with the PEI of the higher molecular weights (curves c and d). A clear second order maximum is present in the reflectivity curve of PEI-600-retinoate, which proves the assumptions of a lamellar structure of the complex. The long periods of the structures in the films are 3.3 nm (PEI-600), 3.4 nm (PEI-2000), 3.4 nm (PEI-25000) and 3.6 nm (PEI-750000). Within the experimental errors these values are in good agreement with those determined for the structures of the complexes in bulk form.

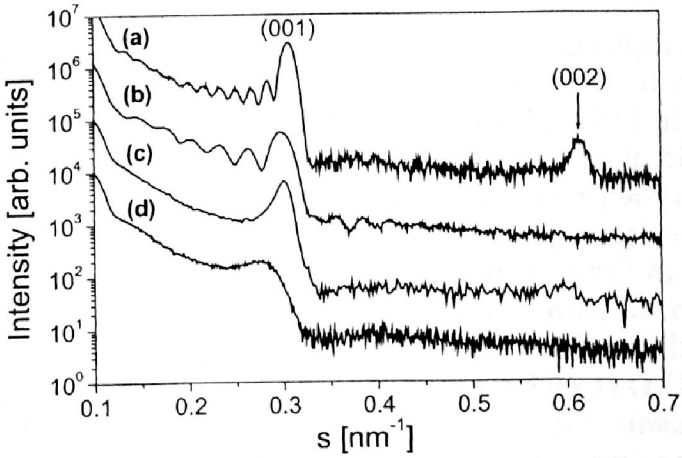

Fig. 25 X-ray reflectivity curves of thin films of PEI-retinoate complexes at the silicon wafer surfaces. The molecular weights of the PEI used for complexation are 600 g/mol (*a*), 2000 g/mol (*b*), 25000 g/mol (*c*) and 750000 g/mol (*d*). Reprinted with permission from [179]. Copyright 2000 American Chemical Society

Because the same mesomorphous structure was developed in a slow film forming process (solvent casting) and in a fast film forming process (spin coating), it was concluded that the time which is necessary for the formation of the mesophase is shorter than the time necessary for the formation of films. The latter is in the order of one second. The thicknesses of the films formed by the lower molecular weight PEIs were 80±2 nm (PEI-600) and 47±2 nm (PEI-2000) as calculated from the angular positions of the fringes [185]. The reflectivity curves were explained as resulting from about 25 (PEI-600) and 15 double layers (PEI-2000) respectively. Here the double layer is defined as a structure building block with an ionic sheet covered by nonionic sheets. The latter are formed by the tails of the retinoic acid. In contrast to the complexes of the lower molecular weight PEI, the film surfaces obtained by the complexes of the higher molecular weight PEIs are not sufficiently smooth to produce Kiessig fringes in their reflectivity curves. The correlation length of the lamellar structure in the direction vertical to the wafer surface was determined, from the width of the Bragg peaks, to be 66±5 nm (PEI-25000) and 32±5 nm (PEI-750000). The structure of the films can be explained as consisting of multi-layers aligned parallel to the wafer surface.

The observation of the macroscopic orientation of the complexes to multi-layers with a variability in their order which were produced in a single-step procedure represents a significant step in the progress of using self-assembly for the preparation of thin organic films. Mechanical fields, present at the spin coating procedure, are probably the reason for the macroscopic orientation of the lamellar stacks parallel to the underlying substrate surface. Such films, when highly loaded with an effective drug, may be useful as a colloidal pharmaceutical formulation.

3.3.3.3 Release Properties

Films of the complexes are stable in water at a pH of 7 while they dissolve at pH 5. This can be explained by the pK_a value of retinoic acid, which is, for example, 6.05 in 150 mM NaCl and 6.49 in 5 mM NaCl [163]. Therefore, the anionic retinoic moieties within the complexes will be protonated at pH values lower than the pK_a which lead to the cleavage of the ionic bonds in the complexes. The first experiments to evaluate the release properties of retinoic acid from thin films of the complexes were performed by using FTIR and surface tension measurements. Films were immersed in solutions of 0.15 m sodium chloride at pH 5 for both methods. The increase of the absorbance at 1255 cm^{-1} (C-O stretch vibration) [186] in the FTIR spectra was used as a qualitative measure for the release of retinoic acid from the PEI-retinoate complexes. For comparison, the spectra of the complex and of the non-complexed retinoic acid are shown at wave numbers around 1255 cm^{-1} (Fig. 26, insert curves a and b). The time-dependency of the absorbance, which is a relative measure of the amount of released retinoic acid, is shown in Fig. 26. It can be seen that the increase of the absorbance, and therefore the release

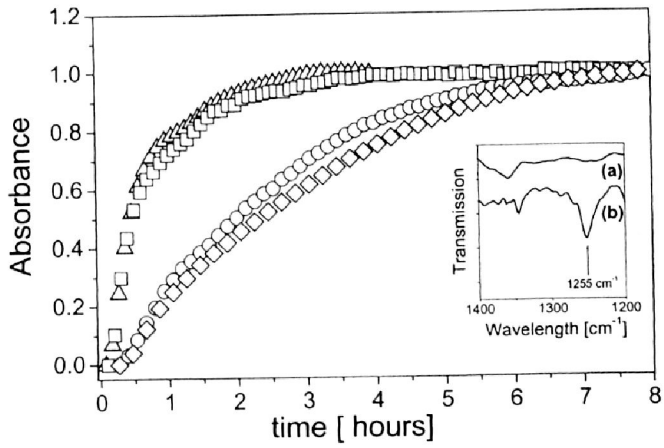

Fig. 26 Time-dependency of the FTIR spectra of the PEI retinoate complexes at a wave number of 1255 cm^{-1}. The samples are PEI-600 retinoate (diamonds), PEI-2000 retinoate (*circles*), PEI-25000 retinoate (*squares*) and PEI-750000 (*triangles*). The *insert* shows the transmission of a complex (*a*) and of non-complexed retinoic acid (*b*) around a wavelength of 1255 cm^{-1}. Reprinted with permission from [179]. Copyright 2000 American Chemical Society

of retinoic acid from the complexes, increases in the line PEI-600, PEI-2000, PEI-25000, PEI-750000.

Obviously the release from the complexes with the higher molecular weight PEIs is faster than that from the complexes with the lower molecular weight PEIs. Because the ratio of primary to secondary to tertiary amino functions in all PEIs is approximately the same, it was suggested that the different release profiles probably originate from the different supramolecular ordering of the complexes and are not due to the minor differences in their molecular composition. Together with the results from the X-ray reflectivity measurements it has been concluded that the release of retinoic acid from a complex film is relatively slow for the higher ordered films and relatively fast for the less ordered films. This explains why the release from the complexes with higher molecular weight PEIs is faster than it is from the complexes with the lower molecular weight PEIs.

The molecular structure of retinoic acid is typical for an amphiphilic compound that is concentrated at interfaces. Further, the carboxylic acid groups allow such compounds to adjust their amphiphilic character by the degree of their dissociation. Surface tension measurements were carried out in order to determine the surface activity of retinoic acid [179]. The surface tension with respect to the concentration at pH 5 decreases more strongly than at pH 9. This reflects the fact that the protonated form of retinoic acid is more efficient in its surface activity than the deprotonated form. The critical micelle concentrations are 3.7±0.5 mg/L (pH 5) and 19±2 mg/L (pH 9). The limiting surface tension values in both curves is about 35 mN/m. Due to the precipitation of retinoic acid, the highest concentration in the surface tension curve at a pH of 5 was 20 mg/L. By contrast the solubility at pH 9 is at least 1 g/L. In order to verify the results from the FTIR measurements, films of the complexes were immersed in a solution of 0.15 mol/L sodium

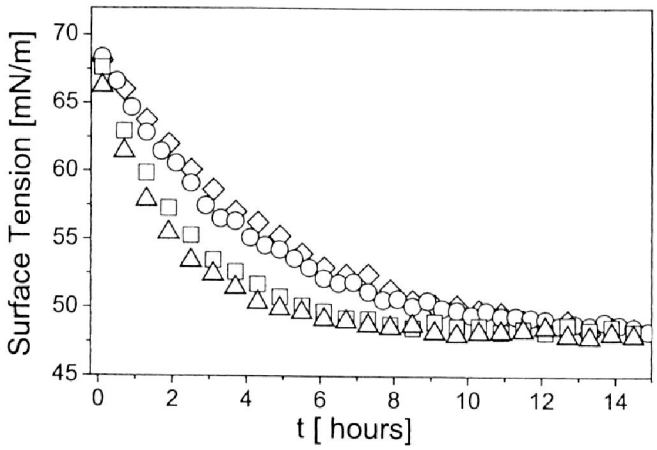

Fig. 27 The effect of the molecular weight of PEI retinoate complexes on the surface tension of 0.15 m/L sodium chloride solutions as a function of time. The samples are PEI-600 retinoate (*diamonds*), PEI-2000 retinoate (*circles*), PEI-25000 retinoate (*squares*) and PEI-750000 retinoate (*triangles*). Reprinted with permission from [179]. Copyright 2000 American Chemical Society

chloride at pH 5. It can be seen in Fig. 27 that the surface tension decreases with time when the films were inserted in the solutions. The decrease is steeper the higher the molecular weight of the PEI is. The final value of the surface tension for all films is around 48 mN/m. This corresponds to a maximum concentration of about 2 mg/L, which is below the critical micelle concentration for retinoic acid. We interpret the reduction of the surface tension to be due to the release of retinoic acid from the films. The release is faster for the higher molecular weight PEI complexes than for the lower. Because the limiting values of the surface tensions are independent of the molecular weight of the PEIs, it was concluded that the kinetics of the release are affected by the PEI used, but not the overall amount of released retinoic acid. This is consistent with the results from the FTIR spectroscopy, and with the assumption that the complexes differ only in their supramolecular orders.

3.3.3.4 Nanoparticles

The formation of the nanoparticles of the complexes was carried out with the aid of poloxamer 188, a triblock copolymer, consisting of two polyethyleneoxide blocks and a polypropyleneoxide block (see Fig. 12). The diameters of the particles, as determined by dynamic light scattering, are shown in Fig. 28. Surprisingly, the diameters decrease with the increasing molecular weight of the PEI as follows: 580 nm (PEI-600), 240 nm (PEI-2000), 185 nm (PEI-25000), 160 nm (PEI-750000). The polydispersities are about 0.25. The sizes were checked by electron microscopy (not shown). Park and Choi [187] have shown that the structures of the PEIs are randomly branched but they become more compact with increasing molecular weight. Probably the

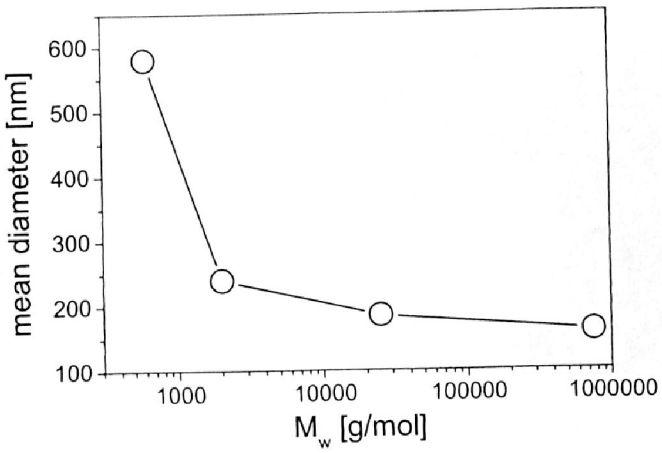

Fig. 28 The molecular weight dependency of the mean diameter of particles of the PEI-retinoate complexes. The molecular weight is the weight average of the PEI used for complexation. Reprinted with permission from [179]. Copyright 2000 American Chemical Society

unexpected size-dependency of the nanoparticles reflects the structural properties of branched PEI. On the basis of this hypothesis it must be expected that PEI-750000 retinoate forms a significantly more compact particle structure than PEI-600 retinoate. AFM measurements, carried out on dried PEI retinoate particles, confirmed the expectation of an increase in compactness of the particles with increasing molecular weight. Examples are shown in Fig. 29. It was found that the higher the molecular weight of the PEI, the more compact the particles. The height profiles of PEI-750000 retinoate (Fig. 30b), for example, are those of typical rigid spheres. The diameters of the particles determined by AFM are about 50 nm smaller than those determined by dynamic light scattering. The higher radii in solution can be explained as an effect of the Poloxamer corona that surrounds the particles, which is swollen in aqueous solution, leading to higher radii in solution than in the dry state. The AFM pictures of the PEI-600 retinoate nanoparticles are unique in their appearance. Here, the particles are collapsed and surrounded by crystalline Poloxamer 188. For comparison the pure Poloxamer, which was prepared from aqueous solution on mica in the same way as the particles, was investigated. It can be seen in Fig. 29d that Poloxamer 188 forms structures which are very similar to those found in the corona of the particles in Fig. 29a. A characteristic detail of the PEI-600 retinoate particles is that there are holes in the centers of many of them. These are indicated in the 2×2 μm large bird's eye view of Fig. 29b, pointed by arrows. A typical cross-section profile is shown in Fig. 29a. Obviously, the PEI-600 retinoate particles in solution were not homogeneous spheres. Probably these particles may have a doughnut-shape-or toroid-structure in solution, such as described recently by Förster et al. for polyelectrolyte block copolymer micelles [188]. A different morphology of the PEI-600 retinoate particles can explain why the mean diameter of the particles is significantly higher than that of the other complexes.

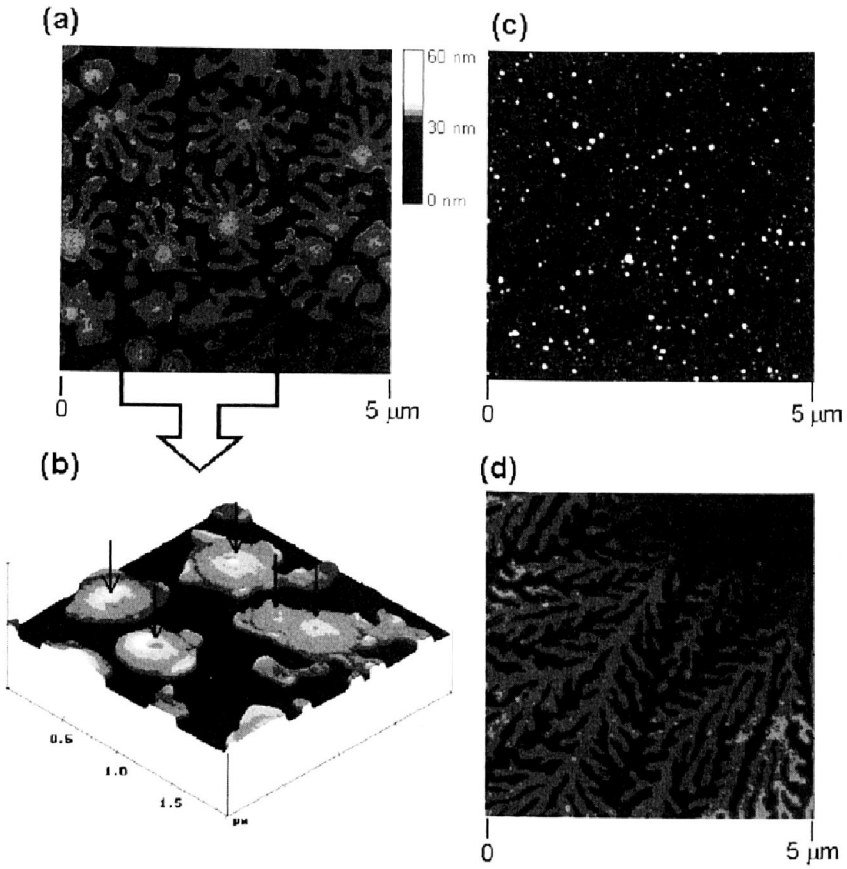

Fig. 29 AFM images of PEI-retinoate particles dried on mica surfaces. (**a**) and (**c**) are top-view images of the PEI-600 retinoate and the PEI-750000 retinoate, respectively. The bird's-eye view (**b**) is a magnification of (**a**) enclosed in the *plotted rectangle*. *Arrows* in (**b**) indicate the depressions in the center of the particles. (**d**) is the top view of Poloxamer 188 after the aqueous solution had been dried out. Reprinted with permission from [179]. Copyright 2000 American Chemical Society

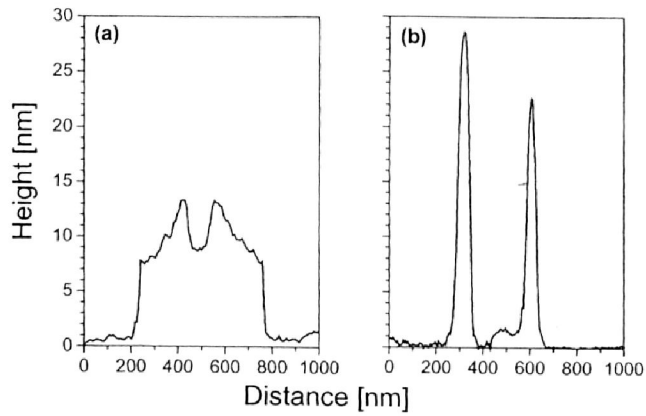

Fig. 30 Height profiles of the cross section of nanoparticles formed by PEI-600 retinoate (**a**) and PEI-750000 retinoate (**b**). Reprinted with permission from [179]. Copyright 2000 American Chemical Society

In conclusion, it was shown that the complexes formed by PEI and the amphiphilic drug retinoic acid are lamellar structured materials, which can be processed as lamellar layered ultra-thin films as well as nanoparticles. The film forming properties of the complexes are the better the lower the molecular weight of the PEI is. All complexes are stable in physiological saline at pH 7, whereas retinoic acid is released at pH 5. The higher the molecular weight, the faster its release. With the help of a water-soluble block copolymer, nanoparticles were formed, the size of which decreases with the increasing molecular weight of the PEI. This was explained as a phenomenon induced by the pristine PEI structure. The shapes of the particles from the complexes of the high molecular weight PEI are compact spheres, whereas those of the lowest molecular weights are probably of doughnut-shape or toroid structure.

4 Theory of Polyelectrolyte Complexation

Although the experimental body of work on polyelectrolyte complexation is very large, there are very few quantitative theoretical approaches. If the polyelectrolytes are weakly charged which is not the case in most of the experiments discussed in this review, the electrostatic interactions are weak and a theory similar to the Debye-Hückel theory of electrolytes can be proposed. This was first done by Borue and Erukhimovich [189]. In this short section, we review the results that have been obtained for the phase diagram of symmetric polyelectrolyte complexes [190], for polyelectrolyte multilayers [191] and for block-polyampholytes which are diblock copolymers with one sequence carrying positive charges and one sequence carrying negative charges [192]. Finally we briefly describe the concept of the effective interaction between two polyelectrolyte complexes.

4.1 Debye-Hückel Theory of Polyelectrolyte Complexes

In a simple mean field theory, the charge density in an electrolyte solution vanishes and the electrostatic contribution to the free energy of the solution also vanishes. The electrostatic free energy is therefore an effect of the charge density fluctuations. The starting point of the Debye-Hückel theory of electrolytes is to assume that these fluctuations are small and can be treated as an expansion which is limited to quadratic order in the free energy. We use here the same description for polyelectrolyte complexes. It is consistent only if the fractions of charged monomers f_+ and f_- on the two polymers forming the complex are small. A polyelectrolyte complex in solution is at least a 5 component system comprising the solvent, the two polymers at concentrations c_+ and c_- and their respective counterions at concentrations n_- and n_+. We consider as counterions any small ions in the solution; if there is added salt, its ions have the same chemical nature as the polymer counteri-

ons. The only constraint on the concentrations is then the macroscopic electroneutrality of the solution, $n_+ + c_+ = n_- + c_-$. For a sake of simplicity, we consider here only symmetrical complexes where the same very large number of monomers N, the same fraction of charged monomers f and the same concentrations, $c_+ = c_- = c$ and $n_+ = n_- = n$.

The calculation of the electrostatic free energy is done by expanding the solution free energy in a given configuration at lowest order in powers of the 4 concentration fluctuations and then by summing over all possible concentration fluctuations. As an example, we discuss first here the simple case where the added salt density is large (n>>c). We define the Debye Hückel screening length counting only the small ions as $\kappa^2 = 8\pi\ {}_B n$ where $l_B\ q^2/(4\pi\varepsilon kT)$ is the so-called Bjerrum length. The electrostatic interactions are attractive and provoke the precipitation of the complex. The precipitation gives a phase separation between the complex phase rich in polymer and a dilute phase containing essentially no polymers but containing small ions (salt). The results are very similar to the standard Debye-Hückel theory, the electrostatic osmotic pressure difference between the complex and the dilute phase can be written as $\Pi_{el} = -kT/\xi_{el}^3$ where ξ_{el} is the electrostatic correlation length given by

$$\xi_{el} \sim \frac{\kappa a}{(4\pi l_B f^2 c)^{1/2}} \tag{3}$$

At equilibrium the osmotic pressure is equal in the two phases and the electrostatic osmotic pressure is balanced by the excluded volume osmotic pressure in the complex that for Gaussian polymers (at the θ point) reads $\Pi_{ev} = w^2 c^{3/2}$. The concentration in the complex then reads

$$c_{comp} \sim \frac{f^2}{a^2 n\, w^{3/4}} \tag{4}$$

It increases with the charge of the polymers and as expected, decreases with the ionic strength. So far, we have ignored the translational entropy of the polymer chains that tends to zero in the limit where N tends to infinity. If N is smaller, the translational entropy of the polymer chains must be included in the pressure balance and stabilizes a homogeneous solution when it becomes of the order of the electrostatic attractive pressure. Complex formation thus only occurs if

$$\frac{n^2 a^2 w^{3/4}}{N f^4} < 1. \tag{5}$$

If the molecular weight is too small or if the fraction of charged monomers is too low, the mixture of positively charged and negatively charged polyelectrolytes is soluble in water.

A more detailed study of the phase diagram of the polyelectrolyte complex must take into account the non-electrostatic interactions between the two polymers characterized by the Flory interaction parameter χ. This inter-

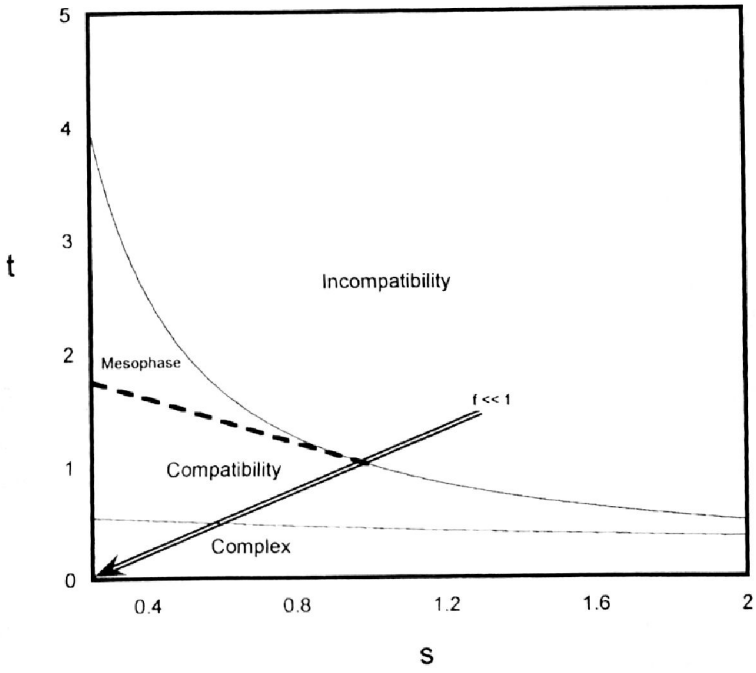

Fig. 31 Theoretical phase diagramm for a symmetric mixture of positive polyelectrolytes. s measures the effect of ionic strength and t that of the incompatibility

action most often leads to a macroscopic phase separation into two phases each containing mostly one of the polymers. There is thus a competition between a complexation transition and a demixing transition. In order to have a qualitative idea of the phase diagram, we have calculated the concentration correlation matrix in the solution at the same level of approximation (the so-called one-loop approximation in the field theory language). The signature of a phase transition is a divergence of this matrix. For the complexation transition, the order parameter is the total polymer concentration $c_+ + c_-$ and for the demixing transition it is the charge density $\rho = c_+ - c_-$. The spinodal line associated to the phase transitions occurs when the corresponding correlation function diverges in the macroscopic limit of zero wave vector. We also looked for divergences at finite wave vectors that corresponds to the formation of mesophases in the solution where the polymer composition of the solution oscillates periodically with space. The theoretical phase diagram for a symmetric mixture of positive polyelectrolyte is presented in Fig. 31. The two dimensionless variable are

$$s = \left(\frac{4\pi l_B}{f^2 c}\right)^{1/2} n a, \quad t = \frac{\chi}{a(4\pi l_B f^2 c)^{1/2}}, \tag{6}$$

s measures the effect of ionic strength and t that of the incompatibility, all other quantities being kept constant. There are 4 phases, a complex phase at low values of χ, a demixing region at high values of χ, a homogeneous solution, and a mesophase region at small ionic strength and intermediate χ. If the fraction of charged monomers is increased as in the experiments of Dja-

doun et al. [193], at low fraction of charged monomers, the solution demixes into two phases it then becomes homogeneous and at large fraction of charged monomers, it forms a complex as indicated by the arrow.

4.2 Polyelectrolyte Multilayers

Over recent years, a major development in the field of polyelectrolyte complexes has been the introduction of polyelectrolyte multilayers by Decher [194]. Some of their properties are described in this paper and they have become one of the very efficient and versatile ways of making surface coatings. We very briefly discuss here the implications of the Debye-Hückel properties of polyelectrolyte complexes for the formation of polyelectrolyte multilayers.

The first layer is obtained by adsorbing a polyelectrolyte layer (say with a positive charge) on an oppositely charged substrate (a negative substrate). One wants to strongly inverse the substrate charge upon adsorption [195] and this may require a non-electrostatic attraction between polyelectrolyte and substrate. The first layer is, for this reason, often made of another polyelectrolyte than the rest of the build up. We assume here that the structure of this adsorbed layer is the thermodynamic equilibrium structure and that it is made at a given high ionic strength (a salt concentration n). For the rest of the build up, we will suppose that the multilayer is never dried and that it is always in contact with an ionic solution at the same ionic strength. This is not how the layers are made in practice but this insures that the polymer remains liquid and close to thermodynamic equilibrium at each step. We also assume that the adsorption is irreversible in the sense that the adsorbed polymer amount remains constant but that the polymer chain conformations at each step can equilibrate. The polyelectrolyte is then in a constrained thermodynamic equilibrium. We call Γ_1 the adsorbed monomer amount in the first layer per unit area.

After rinsing in a salt solution, the first layer is put in contact with a dilute solution of polyelectrolyte of opposite charge at the same ionic strength (negatively charged). The negatively charged polymer in the solution forms a complex that neutralizes the already adsorbed positively charged polymer (as above, we only consider the symmetric case where the two polymers have the same degree of polymerization and the same fraction of charged monomers). The density of this complex is equal to the density c_{comp} of a symmetric polyelectrolyte complex in solution. However there is an excess of negatively charged polyelectrolyte in the solution and the negatively charged polyelectrolyte can form loops dangling from the multilayer into the solution. The loop structure is very similar to that of an adsorbed polymer layer and the monomer concentration in this loop layer decays as $c(z)-1/(z+d)^2$ from the edge of the multilayer. The charge of this loop layer overcompensates the charge of the originally adsorbed polymer, it allows for a new charge inversion and can serve to complex the following layer. The quantity of monomers in this non compensated layer is

$$\Delta\Gamma \sim \frac{1}{w^{2/3}}\left[1 - \frac{f^2}{n^{3/2} l_B^{1/2} a^2 w^{2/3}}\right]. \tag{7}$$

The build up process can the be iterated and at each step the amount of polymer added to the layer is of order $\Delta\Gamma$. It increases weakly with ionic strength. This is in qualitative agreement with the experiments of Laddam et al. [196] that were performer in conditions that are as close as possible as the one described here.

This approach is a purely thermodynamic approach in the sense that locally, the polymer is at thermal equilibrium. The density inside the layer is homogeneous and is equal to the complex density c_{comp}. One of the important experimental results is that, in the multilayers, each layer strongly intermixes with its neighbors but that it keeps its identity in the sense that it does not mix with layers far apart. This "freezing" of the structure must be due to an extremely slow diffusion between the layers that our model is not able to study.

4.3 Block Polyampholytes

Another interesting application of the complexation model is to block polyampholytes. These are diblock copolymers composed of a positive polyelectrolyte block of N_P monomers and a negative polyelectrolyte block of N_M monomers. If the two blocks are symmetric (same molecular weight and same fraction of charged monomers), a copolymer solution precipitates as a standard polyelectrolyte complex, the connection between the two chains playing only a small role. If the copolymer is very asymmetric, $N_P >> N_M$ it can form aggregates such as spherical micelles. The core of the micelle is made of the negative block and of N_P monomers of the positive block and has a concentration c_{comp}; the corona of the micelles is made of the $N_P - N_M$ remaining monomers, it behaves as a polyelectrolyte corona [197]. The geometrical characteristics of these micelles can then be calculated using a standard theory of micellization that estimates independently the free energies of the two blocks. We find an aggregation number

$$P \sim \frac{N_M^{3/5} f^{16/5}}{\left[n^2 w^{2/3} a^4\right]^{4/5}} \tag{8}$$

It increase with the charge fraction f and decreases with ionic strength. This is consistent with experiments on block polyampholytes where the pH is varied [198].

4.4
Effective Interaction Between Two Polyelectrolyte Complexes

Let us finally discuss the concept of effective interactions between two polyelectrolyte complexes which is particularly useful if the architecture of the complexes is known a priori, for a review, see [199, 200]. One typically starts with two complexes choosing their center-of-mass distance r as the statistical variable which is kept fixed while all other statistical degrees of freedom such as solvent molecules, counter- and salt ions and monomers are integrated out. The resulting quantity $V(r)$ is the (pair) potential of mean force between two complexes which can be used as a further input in a simple many body theory for many complexes at finite concentration. There have been several attempts to calculate the effective pair interaction theoretically, the most widely known is the classical Debye-Hückel theory of counterion screening resulting in screened Coulomb interactions between the charged monomers [201]. Following the standard approach of Oosawa [202], these can be combined with Flory arguments for polymer flexibility, polymer self-avoidance, and counterion condensation along the charged monomers. Another important contribution comes from the translational entropy of the microions.

A variational theory which includes all these different contributions was recently proposed and applied for completely stretched polyelectrolyte stars (so-called "porcupines") [203, 204]. As a result, the effective interaction $V(r)$ was very soft, mainly dominated by the entropy of the counterions inside the coronae of the stars supporting on old idea of Pincus [205]. If this pair potential is used as an input in a calculation of a solution of many stars, a freezing transition was found with a variety of different stable crystal lattices including exotic open lattices [206]. The method of effective interactions has the advantage to be generalizable to more complicated complexes which are discussed in this contribution-such as oppositely charged polyelectrolytes and polyelectrolyte-surfactant complexes-but this has still to be worked out in detail.

References

1. Thünemann A (2002) Prog Polym Sci 27:1473
2. Kötz J, Kosmella S, Beitz T, Prog Polym Sci (2001) 26:1199
3. Bertrand P, Jonas A, Laschewsky A, Legras R (2000) Macrom Rapid Comm 21:319
4. Ober CK, Wegner G. (1997) Advanced Materials 9:17
5. Antonietti M, Burger C, Thünemann A (1997) TRIP 5:262
6. Antonietti M, Thünemann A. (1996) Current Opinion in Colloid & Interface Sci 1:667
7. MacKnight WJ, Ponomarenko EA, Tirrell DA (1998) Accounts Chem Res 31:781
8. Schmidt J, Decher G, Hong JD (1992) Thin Solid Films 210/211:831
9. Decher G (1997) Science 277:1232-1237
10. Lvov YM, Sukhorukov GB (1997) Biologicheskie Membrany 14:229-250
11. Ariga K, Lvov Y, Kunitake T (1997) J Am Chem Soc 119:2224
12. Struth B, Eckle M, Decher G, Oeser R, Simon P, Schubert DW, Schmitt J (2001) European Physical Journal A 6:351

13. Radtchenko IL, Sukhorukov GB, Mohwald H (2002) Colloids & Surfaces A-Physicochemical & Engineering Aspects. 202:127
14. Caruso F (2001) Adv Mat 13:11
15. Antonietti M, Conrad J, Thünemann A (1994) Macromolecules 27:6007
16. Goddard E. D, Colloids Surf (1986) 19:301
17. Hayakawa K., Kwak JCT (1982) J Phys Chem 86:3866
18. Hayakawa K, Kwak JCT (1983) J Phys Chem 87:506
19. Philipp B, Dawydoff W, Linow KJ (1982) Zeitschrift für Chemie 22:1
20. Zezin AB, Kabanov (1982) Usp Khim 51:1447
21. Kabanov VA, Zezin AB (1984) Pure appl Chem 56:343
22. Kabanov VA (1994) In: Dubin P, Bock J, Davies RM, Schulz DN, Thies C (eds) Macromolecular Complexes in Chemistry and Biology. Springer Verlag, Berlin Heidelberg New York, p 151
23. Tsuchida E, Osada Y, Sanada K (1972) J Polym Sci A 10:3397
24. Tsuchida E, Osada Y, Ohno H (1980) J Macromol Sci B 17:683
25. Tsuchida E, Abe K (1982) Adv Polym Sci 45:1
26. Bakeev KN, Izumrudov VA, Kabanov VA (1988) Doklad Akad Nauk SSSR 299:1405
27. Zezin AB, Kabanov, VA (1982) Usp Khim 51(9):1447
28. Izumrudov VA, Kharenko OA, Kharenko AV, Gulaeva ZG, Kasaikin VA, Zezin AB, Kabanov VA (1980) Visokomol Soed A 22:692
29. Pergushov DV, Izumrudov VA, Zezin AB, Kabanov VA (1993) Polymer Science Ser A 35:844
30. Bakeev KN, Izumrudov VA, Kuchanov SI, Zezin AB, Kabanov VA (1988) Doklad Akad Nauk SSSR 300:132
31. Izumrudov VA, Bronich TK, Saburova OS, Zezin AB, Kabanov VA (1988) Makomol Chem Rapid Comm 9:7
32. Dautzenberg, H (2001) In: Radeva T (ed) Physical Chemistry of Polyelectrolytes. Surfactant science series, vol. 99, Marcel Dekker, Inc., p 743
33. Micheals AS, Mir I, Schneider NS (1965) J Phys Chem 69:1447
34. Dautzenberg H, Hartmann J, Grunewald S, Brand, F (1995) Ber Bunsen-Gesell, Conference Proceedings of "Polyelectrolytes Potsdam' 95" 100:1024
35. Kriz J, Dautzenberg H (2001) J Phys Chem 105:3846
36. Buchhammer HM, Lunkwitz K, Pergushov DV (1997) Macromol Symp 126:157
37. Petzold G, Nebel A, Buchhammer HM, Lunkwitz K (1998) Colloid Polym Sci 276:125
38. Brand F, Dautzenberg H (1997) Langmuir 13:2905
39. Karibyants N, Dautzenberg H, Cölfen, H (1997) Macromolecules 30:7803
40. Harrison CA, Tan JS (1999) J Polym Sci Part B Polym Phys 37:275
41. Tan JS, Harrison CA, Caldwell KD (1998) J Polym Sci Part B Polym Phys 36:537
42. Hallberg RK, Dubin PL (1998) J Phys Chem B 102:8629
43. Dautzenberg H, Rother G (1988) J Polymer Sci Polym Phys Ed Part B Polymer Physics 26:353
44. Dautzenberg H, Rother G (1992) Makromol Chem Macromol Symp 61:94
45. Dautzenberg H (2000) Makromol Chem Macromol Symp 162:1
46. Chu B (1991) Laser Light Scattering, 2nd edn. Academic Press, Boston
47. Provencher SW (1982) Comp Phys Comm 27:213
48. Philipp B, Dautzenberg H, Linow KJ, Kötz J, Dawydoff W (1989) Progress in Polymer Science 14:91
49. Dautzenberg H, Koetz J, Linow K J, Philipp B, Rother G (1994) In: Dubin P, Bock J, Davies RM, Schulz DN, Thies C (eds) Macromolecular Complexes in Chemistry and Biology. Springer, Berlin Heidelberg New York, p 119
50. Dautzenberg H, Rother G, Hartmann J (1994) In: Schmitz KS (ed) Macro-ion Characterization from Dilule Solutions to Complex Fluids. ACS Symposium Series 548 ACS, Washington DC p 219
51. Papisov IM, Litmanovich AA (1989) Adv Polym Sci 90:139
52. Dautzenberg H, Linow K J, Rother G (1990) Acta Polymerica 41:98

53. Karibyants N, Dautzenberg H (1998) Langmuir 14:4427
54. Dautzenberg H, Rother G, Linow KJ, Phlipp B (1988) Acta Polymerica 39:157
55. Dautzenberg He, Dautzenberg Ho (1985) Acta Polymerica 36:102
56. Dautzenberg H (1997) Macromolecules 30:7810
57. Dautzenberg H, Karibyants N (1999) In: Noda I, Kokufuta E (eds) Proceedings of the 50th Yamada Conference and Second International Symposium on Polyelectrolytes, Inuyama, Japan. Yamada Science Foundation, Osaka, p 284
58. Dautzenberg H, Karibyants N (1999) MacromolChem Phys 200:118
59. Kabanov A V, Bronich TK, Kabanov VA, Kui Yu, Eisenberg A (1996) Macromolecules 29:6797
60. Harada A, Kataoka K (1997) J Macromol Sci-Pure Appl Chem A34(10):2119
61. Dautzenberg H (2000) Macromol Chem Phys 201:1765
62. Zintchenko A, Dautzenberg H, Tauer K, Khrenov V: (2002) Langmuir 18:1386
63. Dautzenberg H unpublished work
64. Schild HG (1992) Prog Polym Sci 17:163
65. Shibayama M, Tanaka T (1992) Adv Polym Sci 109:1
66. Hirose Y, Amiya T, Hirokawa Y, Tanaka T (1987) Macromolecules 20:1342
67. Matsuo ES, Tanaka T (1988) J Chem Phys 89:1696
68. Beltran S, Baker JP, Hooper HH, Blanch HW, Prausnitz JM (1991) Macromolecules 24:549
69. Lee F, Hsu CH (1998) J Appl Polym Sci 69:1793
70. Dautzenberg H, Gao Y, Hahn M (2000) Langmuir 16:9070
71. Xia J, Dubin PL (1994) In: Dubin P, Bock J, Davies RM, Schulz DN, Thies C (eds) Macromolecular Complexes in Chemistry and Biology. Springer, Berlin Heidelberg New York, p 247
72. Kokufuta E (1994) In: Dubin P, Bock J, Davies RM, Schulz DN, Thies C (eds) Macromolecular Complexes in Chemistry and Biology. Springer Verlag, Berlin Heidelberg New York, p 301
73. Tribet Ch (2001) In: Radeva T (ed) Physical Chemistry of Polyelectrolytes. Surfactant science series, vol. 99, Marcel Dekker, Inc., p 687
74. Kabanov VA, Zezin AB, Izumrudov VA (1987) In: Ovchinnikov Yu A (ed) Progress in Science and Technique. Biotechnology. VINITI, Moscow, 4:159 (in Russian)
75. Dautzenberg H, Karibyants N, Zaitsev Syu (1997) Macromol Rapid Commun 18:175
76. Gorokhova I, Zinchenko A, Dautzenberg H, Zaitsev SYu (2002) Langmuir, submitted
77. Czichocki G, Dautzenberg H, Capan E, Vorlop KD (2001) Biotechnol Lett 23:1303
78. Kabanov AV, Felgner PL, Seymour LW (1998) Self-assembling Complexes for Gene Delivery. Wiley
79. Wolfert MA, Dash PR, Nazarova O, Oupicky D, Seymour LW (1999) Bioconjugate Chem 10:993
80. Garnett MC (1999) Therapeutic Drug Carrier Systems 16:147
81. Kabanov AV, Vinogradov SV, Suzdaltseva YG, Alakhov VY (1995) Bioconjugate Chem 6:639
82. Vinogradov SV, Bronich TK, Kabanov AV (1998) Bioconjugate Chem 9:805
83. Read ML, Dash PR. Clark A, Howard K, Oupický D, Toncheva V, Alpar HO, Schacht EH, Ulbrich K, Seymour LW (2000) Eur J Pharm Sci 10:169
84. Kabanov AV (1999) Pharm Sci Technol Today 2:365
85. Oupický D, Koňá, Č, Ulbrich K, Wolfert MA, Seymour LW (2000) J Controlled Release 65:149
86. Bronich T, Kabanov VA, Marky LA (2001) J Phys Chem B 105:6042
87. Dautzenberg H, Zintchenko A, Konak C, Reschel T, Subr V, Ulrich,K (2001) Langmuir 17:3096
88. Shinoda K, Hayashi T, Yoshida T, Sakai K, Nakajima A (1976) Polymer J 8:202
89. Philipp B, Dautzenberg H, Linow KL, Koetz J (1989) Prog Polymer Sci 14:91
90. Koetz J, Kosmella S (1994) J Colloid Interface Sci 168:505

91. Petzold G, Schwarz S, Buchhammer HM, Lunkwitz K (1997) Angew Makromol Chem 253:1
92. Oertel U, Buchhammer HM, Müller M, Nagel J, Braun HG, Eichhorn KJ, Sahre K (1999) Macromolecular Symposia145:39
93. M. Müller (2002) ATR-FTIR Spectroscopy at Polyelectrolyte Multilayer Systems. In: Tripathy SK, Kumar J, Nalwa HS (eds) Handbook of Polyelectrolytes and Their Applications. American Scientific (ASP), pp 293-312
94. Reihs T, Müller M, Lunkwitz K (2002) Colloids and Surfaces (in press, 2002)
95. Reihs T and Müller M (2003, in preparation)
96. Kramer G, Buchhammer HM, Lunkwitz K (1997) Colloids & Surfaces A 122:1
97. Buchhammer HM, Petzold G, Lunkwitz K (1999) Langmuir 15:4306
98. Ladam G, Schaad P, Voegel JC, Schaaf P, Decher G, Cuisinier F (2000) Langmuir 16:1249
99. Borue VY, Erukhimovich IY (1990) Macromolecules 23:3625
100. Castelnovo M, Joanny JF (2000) Langmuir 16:7524
101. Müller M (in preparation 2003)
102. Senger B, Voegel JC, Schaaf P (2000) Coll Surf A 165:255
103. Vuillaume PY, Jonas AM, Laschewsky A (2002) Macromolecules 35:5004
104. Müller M (2001) Biomacromolecules 2:262
105. Müller M, Reihs T, Lunkwitz K (2002) Tagungsband des Makromolekularen Kolloquiums, Freiburg, 21-23 February 2002, pp 58
106. Engelking J, Ulbrich D, Menzel H (2000) Macromolecules 33:9026
107. Pinto MR, Schanze KS (2002) Synthesis-Stuttgart (9 Special Issue SI):1293
108. Müller M, Rieser T, Dubin PL, Lunkwitz K (2001) Macromol Rapid Comm 22:390
109. Müller M, Heinen S, Oertel U, Lunkwitz K (2001) Macromol Symposium 164:197
110. Schwarz B, Schönhoff M (2002) Langmuir 18:2964
111. Müller M, Rieser T, Köthe M, Brissova M, Lunkwitz K (1999) Macromol Symp 145:149-159
112. Goddard ED (1986) Colloids and Surfaces 19:301
113. Zhou SQ, Chu B (2000) Adv Mater 12:545
114. Thünemann AF, Schnöller U, Nuyken O, Voit B (1999) Macromolecules 32:7414
115. Thünemann AF, Schnöller U, Nuyken O, Voit B (2000) Macromolecules 33:5665
116. Thünemann AF, Ruppelt D, Burger C, Müllen K (2000) J Mater Chem 10:13
117. Thünemann AF, General S (2001) Macromolecules 34:6978
118. Ruokolainen J, Makinen R, Torkkeli M, Makela T, Serimaa R, Tenbrinke G, Ikkala O (1998) Science 280:557
119. Antonietti M, Neese M, Blum G, Kremer F (1996) Langmuir 12:4436
120. Zhou SQ, Burger C, Yeh FJ, Chu B (1998) Macromolecules 31:8157
121. Thünemann AF, Lochhaas KH (1998) Langmuir 14:4898
122. Behnke M, Tieke B (2002) Langmuir 18:3815
123. Thünemann AF (1999) Adv Mater 11:127
124. Thünemann AF, Ruppelt D (2001) Langmuir 17:5098
125. Faul CFJ, Antonietti M (2002) Chem A Eur J 8:2764
126. Guan Y, Antonietti M, Faul CFJ (2002) Langmuir 18:5939
127. General S, Antonietti M (2002) Angew Chem Int Ed 41:2957
128. Thünemann AF, General S (2000) Langmuir 16:9634
129. Thünemann AF, General S (2001) J Controlled Release 75:237
130. Hentze HP, Khrenov V, Tauer K (2002) Colloid and Polymer Science, published online 26.7.2002
131. Thünemann AF, Wendler U, Jaeger W, Schnablegger H (2002) Langmuir 18:4500
132. Thünemann AF, Sander K, Jaeger W, Dimova R (2002) Langmuir 18:5099
133. Packer L (ed) (1990) Methods in Enzymology, vol 190. Academic Press, San Diego, CA
134. Lewin AH, Bos ME, Zusi FC, Nair X, Whiting G, Bouquin P, Tetrault G, Carroll FI (1994) Pharmaceutical Research 11:192
135. Bourguet W, Ruff M, Chambon P, Gonemeyer H, Moras D (1995) Nature 375:377

136. Zanotti G, D'Acunto MR, Malpeli G, Folli C, Berni R (1995) Eur J Biochem 234:563
137. Jaeger EP, Jurs PC, Stouch TR (1993) Eur J Med Chem 28:275
138. Krezel W, Ghyselinck N, Samad TA, Dupe V, Kastner P, Borelli E, Chambon P (1998) Science 279:863
139. Zanotti G, D'Acunto MR, Malpeli G, Folli C, Berni R (1995) Eur J Biochem 234:563
140. Thünemann A (1997) Langmuir 13:6040
141. Thünemann AF (2002) European Patent 1 003 559 and US Patent 6 395 284
142. Thünemann AF, Beyermann J, Ferber C, Löwen H (2000) Langmuir 16:850
143. Ponomarenko EA, Tirrell DA, MacKnight WJ (1998) Macromolecules 31:1584
144. Wenzel A, Antonietti M (1997) Adv Mater 9:487
145. Harada A, Cammas S, Kataoka K (1996) Macromolecules 29:6183
146. Bradbury E M, Crane-Robinson C, Goldman H, Rattle HWE (1998) Biopolymers 6:851
147. Botelho LH, Gurd FRN (1976) In: Fasman GD (ed) Handbook of Biochemistry and Molecular Biology, vol 2, 3rd edn. CRC Press: Cleveland, p 689
148. Lide DR (ed) Handbook of Chemistry and Physics, 73rd edn. CRC Press, Boca Raton, 1992
149. Stam CH (1972) Acta Crystallogr 28:2936
150. Douglas SJ, Davis SS (1985) J Colloid Interface Sci 103:154
151. Lechmann T, Reinhart WH (1998) Clin Hemorheol Microcirculat 18:31
152. Pons M, Garcia ML, Valls O (1991) Colloid Polym Sci 269:855
153. Thünemann AF, Beyermann J, Kukula H (2000) Macromolecules 16:5906
154. Allen C, Maysinger D, Eisenberg A (1999) Colloids and Surfaces B: Biointerfaces 16:3
155. Katayose S, Kataoka K (1996) In: Ogata N, Kim SW, Feijin J, Okando T (eds) Advanced Biomaterials in Biomedical Engeneering and Drug Delivery System. Springer, Berlin Heidelberg New York, p 319
156. Kataoka K, Togawa H, Harada A, Yasugi K, Matsumoto T, Katayose S (1996) Macromolecules 29:8556
157. Katayose S, Kataoka K (1997) Bioconjugate Chem 8:702
158. Harada A, Kataoka K (1995) Macromolecules 28:5294
159. Yokoyama M, Okano T, Sakurai Y, Ekimoto H, Shibazaki C, Kataoka K (1991) Cancer Res 51:3229
160. Kwon GS, Suwa S, Yokoyama M, Okano T, Sakurai Y Kataoka K (1994) J Controlled Release 29:17
161. Bronich TK, Nehls A, Eisenberg A, Kabanov VA, Kabanov AV (1999) Colloids and Surfaces B: Biointerfaces 16:243
162. Point JJ (1997) Macromolecules 30:1375
163. Han CH, Wiedmann TS (1998) International Journal of Pharmaceutics 172:241
164. Talibuddin S, Wu L, Runt J, Lin JS (1996) Macromolecules 29:7527
165. Dosiere M (1997) Macromol Symp 114:51
166. Shmueli U, Traub W (1965) J Mol Biol 12:205
167. Elliott A, Malcolm BR, Hanby WE (1957) Nature 179:960
168. Ponomarenko EA, Tirrell DA, MacKnight WJ (1996) Macromolecules 29:8751
169. Thünemann AF, Lochhaas KH (1999) Langmuir 15:4867
170. Antonietti M, Radloff D, Wiesner U, Spiess HW (1996) Macromolecular Chemistry and Physics 197:2713
171. Scheraga HA, Mattice WL (1987) Encycl Polym Sci Eng 7:685
172. Richardson JS, Richardson DC (1989) Prediction of Protein Structure and the Principles of Protein Conformation; Plenum Press: New York, pp 1-98
173. Ruokolainen J, Mäkinen R, Torkkeli M, Mäkelä T, Serimaa R, ten Brinke G, Ikkala O (1998) Science 280:557
174. Kataoka K, Ishihara A, Harada A Miyazaki H (1998) Macromolecules 31:6071
175. Greenfield N, Fasman GD (1969) Biochemistry 8:4108
176. Chou PY, Scheraga HA (1971) Biopolymers 10:657
177. Noy N (1992) Biochimia et Biophysica Acta 1106:159
178. Noy N (1992) Biochimia et Biophysica Acta 1106:151

179. Thünemann AF, Beyermann J (2000) Macromolecules 33:6878
180. Bougligand Y (1998) In: Handbook of Liquid Crystals, vol 1. Wiley-VCH, Weinheim, pp 409-410
181. Bronich TK, Cherry T, Vinogradov SV, Eisenberg A, Kabanov VA, Kabanov AV (1998) Langmuir 14:6101
182. Wolff T, Burger C, Ruland W (1994) Macromolecules 27:3301
183. Ruland W (1977) Colloid Polym Sci 255:417
184. Thünemann AF, Lochhaas KH (1998) Langmuir 14:6220
185. Holy V, Pietsch U, Baumbach T (1999) Springer Tracts in Modern Physics. High-resolution X-Ray Scattering from Thin Films and Multilayers, vol 149. Springer, Berlin Heidelberg New York
186. Rockley NL, Halley BA, Rockley MG, Nelson EC (1983) Analytical Biochemistry 133:314
187. Park IH, Choi E (1996) Polymer 37:313
188. Förster S, Hermsdorf N, Leube W, Schnablegger H, Regenbrecht M, Akari S, Lindner P, Bottcher C (1999) J Phys Chem B 103:6657
189. Borue V, Erukhimovich I (1990) Macromolecules 23:3625
190. Castelnovo M, Joanny JF (2001) Eur Physical J E 6:377
191. Castelnovo M, Joanny JF (2000) Langmuir 16:7524
192. Castelnovo M, Joanny JF (2002) Macromolecules 35:4531
193. Djadoun S, Goldberg R, Morawetz H (1977) Macromolecules 10:1015
194. Decher G (1997) Science 277:1232
195. Andelman D, Joanny JF (2000) Compt Rend Acad Sci IV 1:1153
196. Ladam G, Schaad P, Voegel JC, Schaaf P, Decher G, Cuisinier F (2000) Langmuir 16:1249
197. Borisov O, Zhulina E (1998) Eur Phys J E 4:205
198. Malthig B, Gohy JF, Jerome R, Stamm M (2001) J Polym Sci B 39:709
199. Hansen JP, Löwen H (2000) Annual Reviews of Physical Chemistry 51:209
200. Likos CN (2001) Physics Reports 348:267
201. Löwen H (1994) J Chem Phys 100:6738
202. Oosawa F (1971) Polyelectrolytes. Marcel Dekker, New York
203. Jusufi A, Likos CN, Löwen H (2002) Physic Rev Lett 88:018301
204. Jusufi A, Likos CN, Löwen H (2002) J Chem Phys 116:11011
205. Pincus P (1991) Macromolecules 24:2912
206. Likos CN, Hoffmann N, Jusufi A, Löwen H (2002) Interactions and Phase Behaviour of Polyelectrolyte Star Solutions (2002) J Phys: Condensed Matter (in press)

Received: November 2002